RSC Advances

REVIEW

View Article Online
View Journal | View Issue

Cite this: *RSC Adv.*, 2024, **14**, 19381

A review on Ag nanoparticles fabricated in microgels

Muhammad Arif, *[a] Abdul Rauf [a] and Toheed Akhter *[b]

In recent years, there has been growing interest in the composites of multi-responsive microgels and silver nanoparticles. This innovative hybrid system harnesses the responsive qualities of microgels while capitalizing on the optical and electronic attributes of silver nanoparticles. This combined system demonstrates a rapid response to minor changes in pH, temperature, ionic strength of the medium, and the concentration of specific biological substances. This review article presents an overview of the recent advancements in the synthesis, classification, characterization methods, and properties of microgels loaded with silver nanoparticles. Furthermore, it explores the diverse applications of these responsive microgels containing silver nanoparticles in catalysis, the biomedical field, nanotechnology, and the mitigation of harmful environmental pollutants.

Received 1st April 2024
Accepted 3rd June 2024

DOI: 10.1039/d4ra02467b

rsc.li/rsc-advances

1. Introduction

Gels are polymer networks with crosslinks that can expand when placed in a compatible solvent.[1,2] Among polymer gels, those that can swell in water are referred to as hydrogels.[3] The crosslinked polymeric structure of gels can be categorized into three classes: (i) macrogels which are characterized by a substantial crosslinked structure with greater diameter from 1 μm,[4] (ii) microgels which consist of 3D-crosslinked network colloidal particles dispersed within a solvent with diameter range in 1 μm to 100 nm,[5] and (iii) nanogels are the third class of gels with 3D-crosslinked structure in diameter ranges of 1 nm to 100 nm.[6] Microgels and nanogels have more advantage over macrogels due to their small size and more surface area.[7,8] The adsorption capacity of microgels is more important than nanogels because a large mesh area is present in microgels as compared to nanogels.[9–11] Recently, there has been a significant increase in the attention directed towards microgels, largely

[a]*Department of Chemistry, School of Science, University of Management and Technology, Lahore 54770, Pakistan. E-mail: Muhammadarif2861@yahoo.com; Muhammadarif@umt.edu.pk*

[b]*Department of Chemical and Biological Engineering, Gachon University, Seongnam-13120, Republic of Korea. E-mail: toheed@gachon.ac.kr*

Muhammad Arif

Dr Muhammad Arif is a Professor (Assistant) in Chemistry at Department of Chemistry, University of Management and Technology, Lahore since 2022. He has been working as lecturer in Chemistry at Department of Chemistry, School of Science, University of Management and Technology, Lahore from 2017 to 2022. He has done PhD in Chemistry from University of The Punjab, Lahore, Pakistan. He obtained his M.Phil in Chemistry and M.Sc in Organic Chemistry degrees from Quaid-i-Azam University Islamabad, Islamabad and Institute of Chemistry, University of the Punjab, Lahore, Pakistan respectively. His research area is synthesis, characterization and applications of metal nanoparticles fabricated in microgels and ligands.

Abdul Rauf

Dr Abdul Rauf was born in 1986. He received his PhD from Dalian University of Technology, China under the direction of Prof. Dr Junwei Ye and Prof. Dr Guiling Ning at State Key Laboratory of Fine Chemicals. After doctoral degree, Abdul Rauf began his independent career at University of Management and Technology Lahore Pakistan, where he is now an Assistant Professor of Chemistry. His current research is focused on metal-based coordination polymers, nanomaterial, antibacterial and photo catalysis materials.

propelled by their impressive utility in various domains like drug delivery,[12] chemical separation,[13] enhanced oil recovery,[14] nanotechnology,[15] sensing,[16] and catalysis.[17–19] This heightened attention can be attributed to their responsive behavior in various solvents.[20,21] This responsiveness is characterized by their capacity to undergo rapid and reversible volume changes in response to minor shifts in environmental factors like temperature,[22] pH,[23] and ionic strength.[24] The utilization of smart microgels in composite forms (metal nanoparticles-smart microgel) is growing rapidly.[25–27] They offer a fascinating combined properties derived from both organic and inorganic materials within hybrid systems.[28–30] The hybrid microgels derived from silver nanoparticles and smart microgels have more importance than other metal nanoparticles containing hybrid microgels due to more potential applications,[31] more stability,[32] and low cast as compared to other noble metals. Therefore, Ag-based hybrid microgels are the most interesting hybrid systems among others.

Ag-based hybrid microgels are generated through the combination of Ag nanoparticles with smart polymer microgels through various procedures.[33,34] Typically, smart polymer microgels serve as micro-reactors to synthesize Ag nanoparticles within their structure through an *in situ* reduction of Ag^+ ions, resulting in the formation of Ag-based hybrid microgels.[35] The size of these Ag nanoparticles can be fine-tuned by manipulating key network parameters of the microgels. Notably, these metal nanoparticles can be effectively stabilized within the microgel network for extended periods.[36] Ag-based hybrid systems exhibit a distinctive combination of characteristics derived from both the Ag nanoparticles and the smart microgels. Furthermore, slight variations in temperature[37] and pH[38] of the medium can modulate the optical properties of plasmonic Ag nanoparticles. These factors affect the swelling and shrinking of the microgels which influence the refractive index of the medium. This intriguing combination of materials finds applications in sensors,[39] catalysis,[40] and drug delivery.[41] Mustafa and his coworkers[42] synthesized poly(*N*-isopropylacrylamide-2-hydroxyethylmethacrylate) P(NIA-HEM) core–shell microgels in a single step through free radical emulsion polymerization. They employed these microgels as microreactors to produce silver nanoparticles (Ag NPs) within the shell region of microgels. Subsequently, these hybrid systems were utilized as catalysts for the reduction of 4-nitrophenol (4NiP) to 4-aminophenol (4AmP) under various conditions in an aqueous environment. The value of observed rate constant (k_{obs}) increased from 0.127 min^{-1} to 0.232 min^{-1} with increasing the temperature from 21 °C to 30 °C respectively. The k_{obs} value decreased after further increasing the temperature. Initially, the kinetic energy (KE) of reactants increases with increasing temperature. Therefore, the reactant molecules rapidly reached the surface of Ag NPs. But after 30 °C, the microgels start to deswelling. Therefore, the diffusion rate of reactant molecules decreases and hence, the k_{obs} value also decreases. Gholamali *et al.*[43] have synthesized Ag nanoparticles loaded carboxymethyl chitosan–poly(vinyl alcohol) CMCS–P(VAl) microgels and applied for drug delivery. They loaded the naproxen (anti-biotic) and studied their releasing effect under various content of Ag nanoparticles and pH of medium. The loading occurred at pH = 2.1 due to swelling state and released at pH = 7.4 due to deswelling. The releasing effect of naproxen decreased with increasing the content of Ag nanoparticles in microgels due to hydrogen bonding between Ag nanoparticles and naproxen.

Some of us have previously reported a review article on Ag-based hybrid microgels up to the year 2015, focusing on advancements in their synthesis, characterization, and applications.[44] Main challenges in this field have included regulating the dimensions and shapes of both microgels and Ag nanoparticles, achieving control over the polydispersity of hybrid microgels, managing potential aggregation of Ag nanoparticles within microgels over time or during their application, addressing the leakage of Ag NPs from the crosslinked polymeric network, and mitigating the loss of catalytic performance upon their reuse. Over the past eight years, significant research works have been reported to overcome these challenges and obtaining Ag-based hybrid microgels characterized by exceptional stability, controlled shapes, and sizes, superior monodispersity, and recoverability. To the best of our knowledge, there is currently no comprehensive review summarizing the advancements made in the field of Ag-based hybrid systems over the last eight years.

According to scopus data, 86 articles are reported on Ag nanoparticles decorated in microgels, but 66 articles have been published after 2015. Therefore, a review article is required containing the latest development on Ag-based hybrid microgels. The objective of this article is to offer a critical overview of the advancements made in the stabilization, fabrication, optical properties, and applications of Ag nanoparticles encapsulated crosslinked polymers over the past eight years. This review aims to contribute to the ongoing progress in this field.

The review article covers various aspects of Ag nanoparticles decorated in microgels. Sections 1 and 2 provide a brief introduction and classifications of silver nanoparticles in smart microgels, respectively. The synthetic approaches for Ag-based hybrid microgels are discussed in Section 3 which have been used for their synthesis. The information related to particles size, structure, and morphology of Ag-based hybrid microgels is

Toheed Akhter

Dr Toheed Akhter, Ph.D., is an Assistant Professor at Gachon University, South Korea, specializing in polymer and porous materials. He completed his Ph.D. jointly from KIAST, South Korea, and Quaid-i-Azam University, Pakistan. Dr Akhter has held postdoctoral positions at KAIST and UNIST, South Korea, and previously served as Assistant and Associate Professor at UMT, Pakistan. His research focuses on synthesizing and characterizing innovative materials for diverse applications.

outlined in Section 4. The optical properties of Ag nanoparticles and stimuli responsive behavior of hybrid microgels are highlighted in Section 5. The potential applications of hybrid microgels are described in Section 6 along with enhancing factors in catalysis. Lastly, Section 7 summarizes the conclusions drawn from the discussed findings and suggests future research directions.

2. Classifications of Ag NPs decorated microgels

The morphology of hybrid microgels is very important with respect to their applications. Therefore, Ag NPs encapsulated microgels are categorized into various types depending on the morphologies of hybrid microgels as shown in Fig. 1. These are described below.

2.1. Homogeneous Ag NPs decorated in microgels

In these hybrid microgels, the cross-linking density and content of Ag nanoparticles within the mesh area of the entire hybrid polymeric network is uniform as shown in Fig. 1(a). Such types of silver NPs encapsulated in crosslinked polymers are commonly reported in literature.[45–48] Such hybrid systems exhibit swelling and deswelling behavior in response to appropriate stimuli. These stimuli responsiveness of hybrid microgels affect catalysis, drug delivery, and adsorption capacity. The catalytic activity, adsorption capacity, and drug delivery by such systems are very calm due to easy diffusion of the reactant species. The stability of such systems is greater in form due to surrounding the Ag nanoparticles by electron donating groups. These hybrid systems are further classified into two categories depending upon the one (monometallic) or two (bimetallic) metal nanoparticles in microgels.

2.1.1. Monometallic NPs decorated in microgels. In such classes, only silver nanoparticles are decorated in microgels with uniform distribution and crosslinking density. Such systems are also commonly described in literature.[49–51] Such systems can easily be synthesized. These hybrid microgels have excellent adsorption capacity, catalytic activity, and a greater amount of drug loading and releasing. Such systems show rapidly sensitivity under various conditions. One of use[34] have synthesized such type of hybrid systems. They employed these synthesized systems for catalytic reduction of congo red (CoR) and methyl orange (MeO) dyes. Shu *et al.*[52] have synthesized the Ag NPs encapsulated poly(*N*-isopropylacrylamide-acrylic acid) P(NIA-AcA) hybrid systems. They synthesized hybrid microgels that showed excellent sensing property towards H_2O_2. Li *et al.*[53] have synthesized similar hybrid systems and employed for reduction of 4NiP. They examined the catalytic efficiency of these systems under different values of temperature. Initially, the catalytic activity increased from 20 °C to 32 °C due to increasing the KE of reactants which increases the diffusion of reactants. After that the rate of reduction started to decrease due to deswelling behavior till 39 °C and then start again due to come out of silver nanoparticles on the surface of microgels.

Such systems require ultra-fast centrifugation for regaining the hybrid microgels after catalysis. During this centrifugation process, some content of Ag nanoparticles is leached from the mesh area of crosslinked network of hybrid systems. Consequently, the catalytic performance of these systems decreases rapidly after recycling. Such hybrid systems are very rarely employed for adsorption of pollutants and drug delivery. Such systems can also be employed to reduce different types of organic pollutants. Their adsorption capacity is also an empty space for research.

2.1.2. Bimetallic NPs decorated in microgels. In these hybrid microgels, one different metal along with silver NPs are present uniformly in the crosslinked polymeric network. These hybrid systems are applicable for catalytic reactions.[35] The catalytic performance of bimetallic NPs encapsulated microgels is superior to monometallic NPs due to synergistic effect[54] Bhol *et al.*[33] have synthesized Ag-, Ag/Au-, and Au-based hybrid microgels and applied these synthesized systems for 4NiP reduction. The catalytic reduction rate of Ag/Au-based hybrid microgels was found to be greater than Ag-, and Au-based hybrid microgels due to synergistic effect. This effect facilitates the transfer the electrons from reducing agent ($NaBH_4$) to oxidizing agent (4NiP). In one from my articles,[55] such bimetallic (Ag/Ni) nanoparticles encapsulated microgels has synthesized and applied as catalyst for reduction of azo dyes. The bimetallic hybrid systems were found to be stable under several conditions of pH and temperature. These factors also affect their catalytic performance.

Such systems have more catalytic effect than monometallic but the justification of morphology of bimetallic systems is difficult. For this justification, advanced techniques are used to identify the morphology of bimetallic systems. They are reported only for certain catalytic reactions while the adsorption, drug delivery, and catalytic conversion of various other organic compounds are available space for the new researchers. Therefore, more research is required on such types of systems.

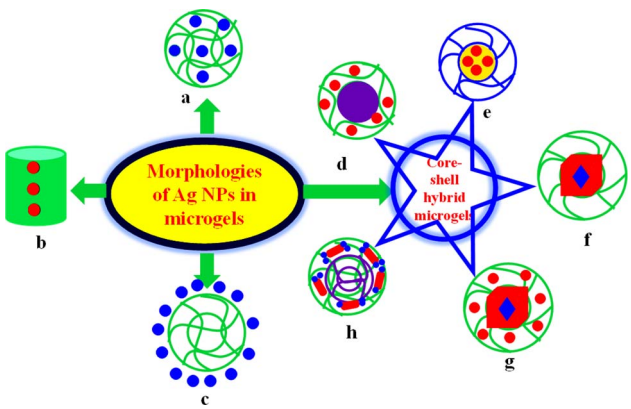

Fig. 1 Classifications of (a) homogeneous hybrid microgels, (b) Ag nanoparticles in hollow tube, (c) microgel encapsulated with Ag nanoparticles, (d) organic core encapsulated with Ag nanoparticles decorated microgels, (e) silica–Ag nanoparticles encapsulated with microgels, (f) bimetallic (Au@Ag) nanoparticles encapsulated with microgels, (g) bimetallic (Au@Ag) nanoparticles encapsulated Ag nanoparticles decorated microgels, (h) organic polymer encapsulated with bimetallic nanoparticles decorated microgels.

2.2. Core–shell hybrid microgels

In such classes, the core region is made up of one type of material and shell with other materials. The core–shell systems have more importance due to their high density, dual behavior, and beauty of designing.[56,57] These hybrid systems are further separated into various systems on the basis of constituting materials of core–shell hybrid microgels.

2.2.1. Organic polymer core encapsulated with Ag NPs decorated in organic shell. In these systems, the core particles are initially generated using appropriate organic materials, followed by the formation of a shell around the core to establish a core–shell polymeric structure as shown in Fig. 1(d). Subsequently, silver (Ag) NPs are incorporated in shell region of core–shell systems. In many instances, both the core regions and the shell consist of crosslinked polymeric network or core consists only organic polymer and shell contains crosslinked organic polymeric network. These types of hybrid systems are further separated into two categories based on mono- and bimetallic NPs which are present into the shell of these core–shell systems.

2.2.1.1. Organic polymer core encapsulated with monometallic NPs decorated in organic shell. In such systems, only silver NPs are present in the shell of core–shell hybrid systems. Such types of hybrid systems are applied for catalytic activity for reduction of different pollutants. Their catalytic efficiency is similar to monometallic homogeneous hybrid microgels, but their density is greater than homogeneous hybrid microgels due to the presence of solid organic core. Nseem *et al.*[58] have synthesized polystyrene@poly(*N*-isopropylmethacrylamide-acrylic acid) P(StR)@P(NIA-AcA) core–shell microgels and then Ag nanoparticles were introduced into the shell region by *in situ* reduction method. They applied these core–shell systems for catalytic reduction/degradation of rhodamine-B (RAmB), brilliant blue (BrB), and methylene blue (MeB) dyes from aqueous medium in separate and simultaneous conditions. The systems showed excellent results for catalytic reduction. Such systems are suitable for reduction of all types of organic pollutants from aqueous medium. Hussain *et al.*[59] have synthesized Ag NPs in polystyrene@poly(*N*-isopropylmethacrylamide-methacrylic acid) P(StR)@P(NIMA-MAcA) core–shell microgels and applied the synthesized hybrid core–shell system for conversion of Cr^{6+} into Cr^{3+} ions. The temperature and pH of medium also affected the catalytic performance of hybrid core–shell systems.

These systems are recycled easily by simple centrifugation processes. Therefore, the leakage of Ag nanoparticles from shell region of core–shell systems is less as compared to homogeneous systems. The Ag NPs are present only in shell of core–shell systems. Therefore, small content of Ag nanoparticles is used in these systems as compared to homogeneous hybrid microgels. In homogeneous hybrid systems, the Ag NPs are present in the center region of hybrid systems, but the reactant molecules reduced by those Ag nanoparticles which are present in outer region of homogeneous microgels. Therefore, inner Ag nanoparticles are not used during catalysis. Such systems are not used for sensing, adsorption, and drug delivery purposes. Such systems have excellent potential for these purposes in the near future.

2.2.1.2. Organic polymer core encapsulated with bimetallic NPs decorated another crosslinked organic polymer shell. In such systems, the core region consists of organic material and shell region also consists of organic polymer with crosslinked network as shown in Fig. 1(h). Ag nanoparticles along with other metal NPs exist in the shell of core–shell microgels. These hybrid systems have more catalytic activity as compared to both (monometallic and bimetallic) homogeneous hybrid microgels and monometallic nanoparticles containing core–shell microgels due to synergistic and easy approachable bimetallic nanoparticles. Such systems also have high density as compared to homogeneous hybrid microgels. Such systems are further classified in two types based on the morphologies of bimetallic nanoparticles. One is bimetallic nanoparticles existing in the shell of core–shell systems and other is core–shell bimetallic NPs present in the shell of core–shell microgels. Both systems have excellent catalytic activity due to synergistic effect. Zhang *et al.*[60] have synthesized P(StR)@P(NIA) systems and then Ag/Pd nanoparticles were loaded homogeneously in shell region of synthesized systems. They applied these systems for 4NiP reduction. The catalytic reduction by bimetallic nanoparticles containing core–shell systems was very fast as compared to monometallic. They also reported that the temperature effect on the catalytic efficiency of hybrid systems. Tan *et al.*[61] have synthesized bimetallic (Au@Ag) NPs loaded in poly(*N*-isopropylacrylamide)@ poly(ethyleneimine) P(NIA)@P(EtI) core–shell hybrid systems and applied as catalyst for 4NiP reductions.

These systems are employed only for catalytic reduction of 4NiP. They can be used for other catalytic reduction reactions. These systems are still not used for adsorption, drug delivery, and sensing purposes. New researchers can work in these fields. They are very important with respect to catalytic reduction reactions due to fast catalytic performance and easy recycling properties.

2.2.2. Inorganic core with Ag nanoparticles encapsulated with organic polymers. In such systems, the core region consists of inorganic materials (SiO_2, Fe_2O_3, or Fe_3O_4) which is surrounded by crosslinked organic polymer and Ag NPs are also present in along with inorganic material in core region as shown in Fig. 1(e). The catalytic efficiency of such hybrids is lower than other systems of core–shell and homogeneous due to the large distance between Ag nanoparticles and reactants. The reactants slowly approach the surface of Ag NPs. Consequently, the reduction rate is very slow. Mohan *et al.*[62] have synthesized such types of hybrid microgels and used for catalytic oxidation reactions of alcohols. The oxidation of aromatic alcohols occurs more rapidly than aliphatic alcohols due to easy electron donating mesmeric effect of benzene ring. Similarly, the oxidation of electron donating groups containing aromatic alcohols happened faster than electron withdrawing containing aromatic alcohols.

These hybrid systems can also be employed for adsorption as well as drug delivery processes. The density of such systems is very high and polar crosslinked network is present for adsorption. This shell region also shows the responsive behavior which

is also an important factor for adsorption and drug delivery with respect to loading and releasing effect.

2.2.3. Metal nanoparticles encapsulated crosslinked organic polymers. In these systems, metal NPs lie in core position which are surrounded with crosslinked polymers. These systems are very important with respect to the stability of metal NPs, but their catalytic efficiency is lower than other systems because the reactants slowly reach to the surface of metal NPs from the bulk region due to large distance. Such hybrid systems are also separated into two types based on one or two metal NPs as shown in Fig. 1(f). Alarcón-Fernández *et al.*[63] have synthesized bimetallic (Au@Ag) NPs encapsulated with crosslinked organic polymer microgels along with other systems. They examined the swelling/deswelling behavior of these systems. Tzounis *et al.*[64] have also synthesized bimetallic (Au@Ag) NPs encapsulated with crosslinked organic polymer. They examined that the catalytic efficiency of bimetallic hybrid systems is superior to monometallic hybrid systems. Metal nanoparticles can be synthesized into the shell region of these core–shell systems as shown in Fig. 1(g). Such systems have better catalytic results than formerly mentioned systems.

Metal NPs in such systems are highly stable but their catalytic activity is very low due to more distance of Ag nanoparticles for reactant molecules. These systems are very useful for drug delivery and adsorption due to the presence of polar crosslinked polymer network and the responsive behavior of this network which helps the loading and releasing the substances. Such systems also have low anti-bacterial activity due to not releasing ability of Ag nanoparticles from hybrid systems.

2.2.4. Metal nanoparticles encapsulated silver NPs loaded organic polymer. In these hybrid systems, the core region consists of metal NPs which are encompassed with crosslinked organic polymers. The shell region of these core–shells is loaded with Ag nanoparticles. Such systems have more catalytic performance than homogeneous hybrid systems and metal nanoparticles encapsulated with organic polymers. Alarcón-Fernández *et al.*[63] have synthesized such systems and examined the Raman scattering effect of these hybrid systems. They did not use these systems for other applications. Tzounis *et al.*[64] also have synthesized such types of hybrid microgels. They employed these synthesized systems as catalyst for 4NiP reduction. The catalytic reduction of 4-nitropheon was occurred as bimetallic nanoparticles encapsulated with Ag nanoparticles loaded crosslinked organic polymer > bimetallic nanoparticles encapsulated with crosslinked organic polymer > monometallic nanoparticles encapsulated with crosslinked organic polymers.

Such systems have excellent catalytic efficiency along with easy recyclable properties. Such systems are also very important for anti-bacterial performance due to easy release of Ag nanoparticles. Such systems are less important for adsorption but important for drug delivery.

2.3. Microgels encapsulated metal NPs

In these systems, microgel is present as core which is surrounded with metal NPs as shown in Fig. 1(c). Such systems have excellent catalytic performance due to the ease reactant molecules approach on the surface of metal NPs. Porosity is generated on the surface of microgels after the introduction of Ag nanoparticles. Therefore, such systems can be used for adsorption processes. Curtis *et al.*[65] have synthesized the crosslinked polymer microgels which is encapsulated with Ag nanoparticles containing borate. The synthesized hybrid system showed pH sensitivity due to the existence of basic groups (amino groups) in their structures.

In this duration, a few articles are reported on such hybrid microgels. These systems are not more appropriate for drug delivery because of the less drug loading. The adsorption capacity of such hybrid systems is low due to occupying the polar surface with Ag nanoparticles. Such systems are more effective for catalytic reactions. They should be applied to reduce other organic pollutants.

2.4. Ag nanoparticles encapsulated with hollow-tube of crosslinked network of organic polymer

In such systems, the silver nanoparticles are present in the mid position which is surrounded by a hallow-tube like crosslinked organic polymer as shown in Fig. 1(b). Such systems are unique with respect to morphologies. Hong *et al.*[66] have synthesized of such type of hybrid systems. They employed these hybrid microgel systems for degradation of toxic CO gas molecules. The hybrid systems showed excellent results for reduction/degradation of CO. These systems are very useful for reducing smoke and flammability toxicity from the environment. These hybrid microgels convert the CO (flammable) to CO_2 (nonflammable) species. In this way, such systems are very important in those places where the chance of flame is maximum because these hybrid microgels reduce this affinity of flame.

More work should be needed in this morphology. These systems can be applied for adsorption, sensing, drug delivery, and catalytic reduction reaction of toxic pollutants from water. This morphology is very important and interesting for new researchers.

3. Synthesis

Several methods have been reported in the literature for the synthesis of hybrid microgels. The method chosen for synthesis is contingent upon the architecture, design, and morphology of the intended hybrid system. Diverse methods employed for the synthesis of hybrid systems as given below.

3.1. Ag nanoparticles synthesis in the dispersion of microgels

Ag nanoparticles can be generated within a dispersion of polymer systems to produce Ag based hybrid systems. This approach is commonly employed to synthesize hybrid systems with a consistent distribution of Ag nanoparticles within the polymer matrix. Initially, microgels are synthesized using a free radical precipitation polymerization method (FRPPM) and then Ag nanoparticles are incorporated either within or onto the microgels through the reduction of salts of metals using an

appropriate reducing agent like $NaBH_4$. Microgel particles serve as microreactors to produce NPs. By manipulating the dispersity and diameter of the pores of polymeric system which control the size and size distribution of Ag nanoparticles. Additionally, the metal content in crosslinked network can be adjusted by varying the composition of the microgel feed. Begum *et al.*[32] have synthesized Ag NPs decorated in poly(*N*-isopropylacrylamide-*co*-acrylamide) P(NIA-AcAm) in two steps as shown in Fig. 2. In the first step, microgel is synthesized by FRPPM and then Ag nanoparticles incorporated by *in situ-reduction* method. The *N*-isopropylacrylamide (NIA) (monomer), acrylamide (AcAm) (comonomer), sodium-dodecyl-sulfate (SoDS) (stabilizer), and *N*,*N*′-methylenebisacrylamide (MeBA) (crosslinker) were added along with deionized water. Then a small amount of ammonium-per-sulfate (AmPS) (free radical initiator) were added to start polymerization. The reaction continued for 4 h under similar conditions. The appearance of milky color indicates the formation of microgels. The product was then dialyzed for purification. In the next steps, a specific amount of Ag salt was added into the dispersion of synthesized microgels under N_2 at room temperature (28 °C). The mixture stirred for one hour and then freshly prepared $NaBH_4$ solution was added to reduce the Ag^+ ions to form Ag nanoparticles. Similar method was reported for synthesis of hybrid microgels by Arif *et al.*[35] and Shahid *et al.*[34]

This method is very simple and easy. The size of Ag nanoparticles is also easily controlled by this method. Therefore, this method is mostly reported in literature. But the drawback of this method is that only homogeneous hybrid microgels can be synthesized.

3.2. Synthesis of hybrid microgels by mixing of Ag NPs and microgel

In such methods, both microgels and Ag NPs are prepared separately, which are subsequently combined to generate Ag nanoparticles-based hybrid microgels. Electrostatic interactions and magnetic stirring play a vital role in the synthesis of these hybrid microgels. The hydrophilic components of the microgel interact with the Ag nanoparticles, allowing the incorporation of Ag nanoparticles into the sieves of microgels through electrostatic attraction. George *et al.*[67] have synthesized hybrid microgels with this method as shown in Fig. 3. They synthesized chitosan–poly(acrylic acid) CS–P(AcA) microgels by using FRPPM. They added chitosan (CS) (monomer), acrylic acid (AcA) (comonomer), *N*,*N*′-methylenebisacrylamide (MeBA) (crosslinker) and deionized water. A small amount of ammonium-per-sulfate (AmPS) (free radical initiator) was then added. The reaction continued for 4 h to complete polymerization. The Ag nanoparticles were synthesized by reduction of Ag salt in the presence of the extract of Euphorbia Maculate. The extract of Euphorbia Maculate reduced the Ag^+ ions into Ag nanoparticles. They can synthesize the Ag nanoparticles-based hybrid microgels by using these Ag nanoparticles and CS–P(AcA) microgels simply by mixing and stirring of both.

In this method, mostly the morphology of hybrid microgels in which microgel encapsulated with Ag nanoparticles are synthesized. The homogeneous hybrid microgels can also be synthesized in microgels when the state of microgels is swelling. In swelling state, the Ag nanoparticles come into the mesh area of microgels. The morphology, in which Ag nanoparticles are present in core and microgels in shell region, cannot be synthesized.

3.3. Microgel synthesized in the solution of Ag NPs

Hybrid microgels with a core–shell morphology in which a metallic core encapsulated with a crosslinked polymeric shell are normally designed by employing pre-existing metal nanoparticles as seed. This type of synthesis is also completed in two steps. In the first step, Ag nanoparticles are synthesized. The polymerization process is conducted within the dispersion of Ag NPs, employing appropriate monomers, crosslinkers, co-monomers, initiators, and surfactants at a specific temperature in the second step. Alarcón-Fernández *et al.*[63] have synthesized bimetallic (Au@Ag)@poly(*N*-isopropymacrylamide) (Au@Ag)–P(NIA) hybrid microgels as shown in Fig. 4. They synthesized Au nanoparticles first by using 3-butanoic acid (reducing agent), benzyldimethylhexadecyl-ammonium-chloride (stabilizer), and Au salts. Ag nanoparticles were synthesized by using Ag salt and ascorbic acid (stabilizer and reducing agent). Then poly(*N*-isopropylacrylamide) microgels were synthesized by using *N*-isopropymacrylamide (NIA) (monomer), allylamine (AlAm) (comonomer), *N*,*N*′-methylenebisacrylamide (MeBA)

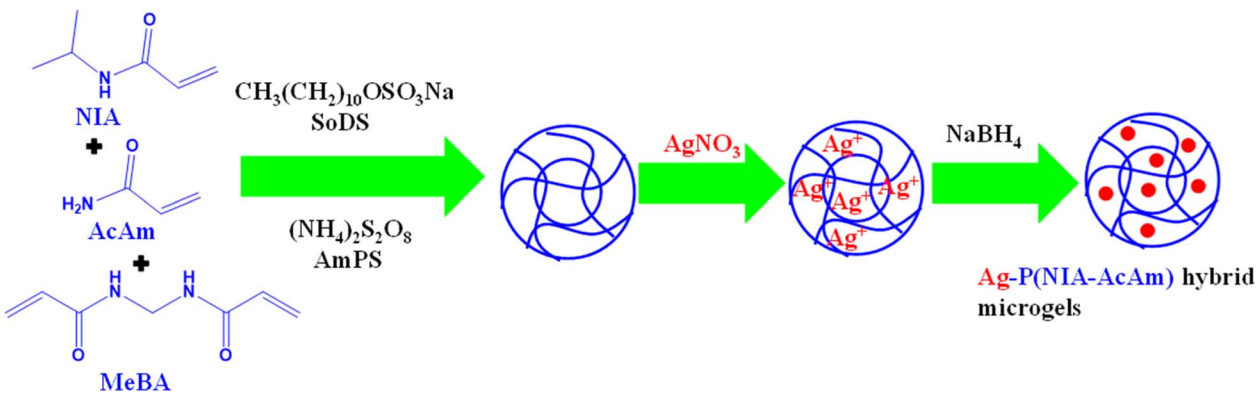

Fig. 2 Pictorial diagram for synthesis of Ag NPs in the presence of poly(*N*-isopropylacrylamide-acrylamide) microgels dispersion.[32]

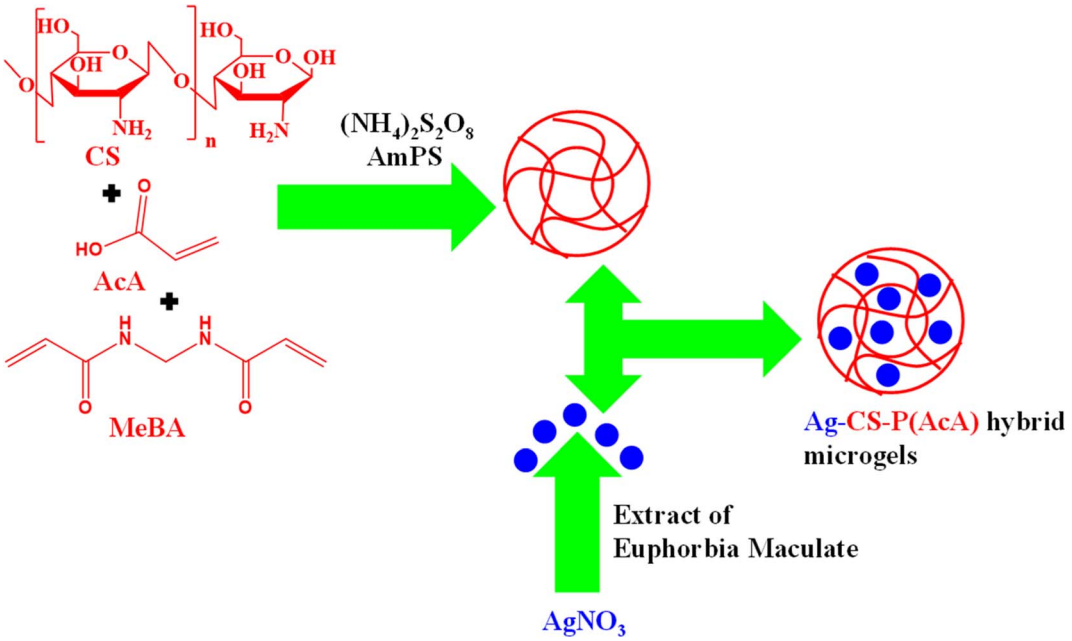

Fig. 3 Synthetic pictorial diagram of Ag NPs decorated chitosan–poly(acrylic acid) hybrid microgels by mixing of Ag NPs and chitosan–poly(acrylic acid).[67]

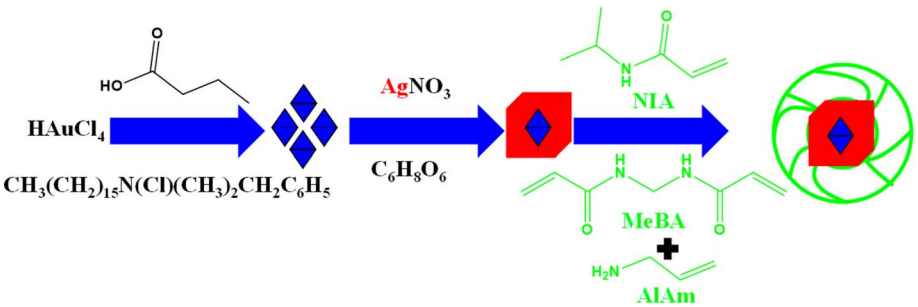

Fig. 4 Synthetic pictorial diagram of poly(*N*-isopropylacrylamide-allylic acid) microgels in the presence of bimetallic (Au@Ag) nanoparticles.[63]

(crosslinker), and 2,2′-azobis(2-methylpropionamidine) dihydrochloride (free radical initiator). Tzounis *et al.*[64] have synthesized bimetallic (Au/Ag) NPs encapsulated Au/Ag–P(NIA) hybrid systems with similar method.

In this method, the core–shell hybrid microgels are synthesized in which Ag nanoparticles are present in the core region. The required size of Ag nanoparticles is difficult to control in this method.

4. Characterizations

The investigation of the size, morphology, structure, and composition of metal NPs decorated in microgels is conducted using various techniques, as summarized in Table 1. These are utilized to differentiate the characteristics of Ag NPs within polymers from those of polymers alone. The analytical techniques encompass Raman spectroscopy (RS),[68] UV-Visible (UV-Vis) spectrometry, ^{1}H Nuclear magnetic resonance spectroscopy (H-NMR), Energy-dispersive X-ray spectroscopy (EDX), Transmission electron microscopy (TEM), X-ray photoelectron spectroscopy (XPS),[69] Field emission transmission electron microscopy (FE-TEM), Fourier transform infrared spectroscopy (FTIR), High-angle annular dark-field scanning transmission electron microscopy (HAADF-STEM), Differential scanning calorimetry (DSC), Dynamic light scattering (DLS),[67] Scanning electron microscopy (SEM), Differential mechanical analysis (DMA), and Atomic force microscopy (AFM).[29] These techniques are employed for the analysis of both the microgels and hybrid microgels. Each characterization technique provides unique insights into the distinct properties of Ag nanoparticles encapsulated crosslinked polymers as compared to crosslinked polymers without Ag nanoparticles. Microscopic technologies, like SEM, HAADF-STEM, TEM, FE-TEM,[41] and AFM, are employed to identify the physical characteristics of both microgels and hybrid systems. SEM technique is utilized to assess the morphology of surface area of both crosslinked polymers and Ag NPs loaded polymers. The size distribution, size, and morphology of microgels and Ag-based hybrid systems are examined using HAADF-STEM, TEM, and FE-TEM techniques. George *et al.*[67] synthesized Ag-based hybrid microgels.

Table 1 Ag NPs decorated smart crosslinked polymers with monomers, metal nanoparticles, morphology and used characterization techniques

System	Metal nanoparticles	Morphology	Characterization techniques	References
Ag–P(NIA-AcA)@NNPA	Ag	Ag NPs in core region of core–shell microgels	AFM, TEM, UV-Vis, PCS	29
(Au@Ag)@Ag–P(NIA)	Ag, Au	Bimetallic (Au@Ag) encapsulated with Ag decorated P(NIA)	TEM, TGA, UV-Vis-NIR, DLS	70
P(StR)@Ag/TiO_2–P(NIA-MAcA)	Ag, TiO_2	P(StR) encapsulated with bimetallic (Ag/TiO_2) NPs decorated P(NIA-MAcA)	EDS, TEM, TGA, XRD, FTIR, UV-Vis, XPS	69
Ag–CS–P(AcA)	Ag	Homogeneous hybrid microgels	FTIR, UV-Vis, DLS, XRD, TEM, *zeta potential*	67
(Au@Ag)@P(HLNA)	Ag, Au	Bimetallic (Au@Ag) encapsulated P(HLNA)	RS, UV-Vis, TEM, WAXD	68
Ag–P(NIA-HEA)	Ag	Homogeneous hybrid microgels	UV-Vis, FE-SEM, SEM, TEM	41
P(StR)@Ag/Pd–P(NIA)	Ag, Pd	P(StR) core encapsulated with bimetallic (Ag/Pd) nanoparticles decorated P(NIA)	DLS, ICP-AES, UV-Vis, SAXP	60
P(EtI)@(Au@Ag)–P(NIA)	Au, Ag	P(EtI) encapsulated with bimetallic (Au@Ag) decorated P(NIA)	AFM, TEM, XPS, *zeta-potential*, UV-Vis, EDS	61
Ag–GL	Ag	Homogeneous hybrid microgels	FE-SEM, XRD, EDX, TGA	71
Ag–P(NIA-MAcA)	Ag	Homogeneous hybrid microgels	UV-Vis, TEM, DLS, FTIR	72

The size of Ag nanoparticles was obtained at 9 nm with TEM, and they are present in the structure of microgels. The stability of these particles checked with UV-Vis spectrophotometer. They found themselves to be stable after three months. Yan *et al.*[69] also synthesized hybrid microgels with varying the content if Ag^+ salt. The size of Ag nanoparticles increased from 5.8 to 10.8 nm with increasing the content of silver salts which are characterized with TEM. Khan *et al.*[41] synthesized 10 nm sized Ag nanoparticles in with *d*-spacing of 0.230 nm and in spherical shape. The stability of Ag nanoparticles remained constant during variation in temperature. The size of microgel and hybrid microgels were found 300 nm and 320 nm respectively in swelling state and these values reduced to 180 nm and 220 nm in deswelling state respectively. Functional groups present in both hybrid microgels and microgels are detected through NMR, FTIR, and RS techniques. Furthermore, the EDX technique is used to find the elemental compositions. XRD is utilized for finding the degree of crystallinity of both microgels and hybrid systems. The influence of external stimuli on the deswelling/swelling behavior of polymers and hybrid polymers is examined using DLS and UV-Vis techniques. The formation, shape (whether spherical or rod-shaped) and stability of Ag NPs in polymeric network are identified through UV-Vis analysis, in conjunction with VFTT. The decomposition, thermal stability, and the percentage of Ag NPs in polymers as compared to crosslinked polymers are identified by DSC and TGA. Additionally, the elemental compositions are ascertained using AFM. The characterization techniques employed to investigate Ag NPs loaded into crosslinked polymers are summarized in Table 1, along with details about the monomers and metal NPs present in the hybrid microgels.

5. Properties of Ag-based hybrid microgels

Hybrid microgels maintain the distinctive characteristics of their constituent elements. As a result, the properties of crosslinked polymers containing Ag nanoparticles can be categorized into two sets: properties stemming from the existence of Ag NPs and properties resulting from the microgel network itself.

5.1. Properties of crosslinked polymeric network

The presence of various functional groups of monomers and comonomers within the structure of microgel imparts specific characteristics to hybrid microgels. The properties of hybrid microgels due to smart microgels is highlighted below.

5.1.1. Temperature sensitivity. The structure of microgels is like a sponge and the interstitial spaces of these microgels can be filled with water molecules. These hybrid microgels display temperature sensitivity as elucidated in the investigations conducted by Arif[11,30,55] and others.[73,74]

The temperature sensitivity of hybrid microgels results due to hydrophilic and hydrophobic interactions within the network of hybrid microgel and with the surrounding water molecules. Typically, hydrophilic interactions predominate over hydrophobic ones at lower temperatures while the reverse occurs with hydrophobic interactions taking priority at higher temperatures. The temperature at which a rapid change occurs in the hydrodynamic diameter (HDD) of microgels is referred to as the volume phase transition temperature (VPTT). A particular type of microgels, which is composed from a single monomer, has a fixed value of VPTT in pure form. For instance, *N*-isopropylacrylamide (NIA)-based systems have a VPTT value of 32 °C. However, this value can be increased by incorporating the hydrophilic groups containing comonomers during the microgel synthesis of microgels. By increasing the content of such hydrophilic comonomers in microgels structure, the interactions between the microgels and water molecules also increase, leading to an elevated VPTT. For example, Yang *et al.*[75] have synthesized NIA-based microgels and determined a VPTT of 32 °C. Nigro *et al.*[76] have investigated by adding the acrylic acid as comonomer in the microgels during synthesis. The value of VPTT raises after the introduction of acrylic acid (AcA). This

addition shifted the VPTT of the microgels from 32 °C to 37 °C, which is approximately equal to human body temperature. This second microgel system is well-suited for drug delivery within the human body due to its VPTT of 37.5 °C. The impact of temperature on the swelling and deswelling behavior of cross-linked polymers is categorized into two distinct types, as described below.

5.1.1.1. Negative temperature effect. In this temperature-related phenomenon, there is an inverse relationship between the value of HDD of microgels and temperature. As the temperature increases, the hydrodynamic diameter of microgels decreases, while it increases as the temperature decreases. This specific temperature effect on the HDD of microgels is referred to as a negative temperature effect. At lower temperatures, strong interactions exist between the polar parts of microgels and water molecules. These interactions start to decrease as the temperature of the medium rises while the hydrophobic interactions gradually become more prominent with increasing temperature. Consequently, water molecules come out from the structure of microgel resulting the decreases in hydrodynamic diameter of microgels. For instance, Li *et al.*[53] Ag nanoparticles loaded poly(*N*-isopropylacrylamide-acrylic acid) Ag–P(NIA-AcA) hybrid systems. They observed the effect of temperature on both microgels and hybrid microgels. The value of HDD decreases as the temperature increases from 20 °C to 50 °C. The value of hydrodynamic diameter is 980 nm at 20 °C and 502 nm at 50 °C. The temperature effect on hybrid microgels is monitored by UV-Vis spectrophotometer. The value of λ_{SPR} shifts to longer wavelength as the temperature increases from 20 °C to 50 °C due to swelling behavior. Similar trends in hybrid microgels are reported by Haleem *et al.*[77] and Tzounis *et al.*[64]

5.1.1.2. Positive temperature effect. In this particular phenomenon, the HDD of hybrid microgels increases as the temperature rises. This occurs because hydrophobic interactions become more pronounced with increasing temperature. Consequently, the microgel particles begin to aggregate, forming larger-sized microgels. Now, an increasing trend is observed in the HDD value of both microgels and hybrid microgels. This behavior of microgels (HDD increases with rising temperature) is referred to as a positive temperature effect. Initially, the hydrodynamic diameter of microgels decreases as the temperature increases due to decreased hydrophilic interaction and enhanced hydrophilic interactions. However, in certain microgels, the HDD of both microgels and hybrid systems starts to increase once again due to coagulation of microgel particles through intermolecular hydrogen bonding. The temperature at which microgel particles begin to coagulate is known as the upper critical solution temperature (UCST). Shah *et al.*[78] also reported similar trend in Ag nanoparticles-based hybrid microgels with increasing the temperature.

5.1.2. Effect of pH. The variations in the swelling and deswelling behavior of microgels under various value of pH in aqueous medium are collectively referred to as the "pH effect". Microgels can be categorized into following types of hybrid microgels due to their acidic or basic nature.

5.1.2.1. Acidic microgels. Such types of microgels possess the ability to release protons from their structure in a basic medium. They are considered acidic in nature because they contain –COOH or $-SO_3H$ groups in their structure. These acidic groups of hybrid microgels release their protons when the pH of the medium is equal to or greater than the pK_a value of the acidic moiety. After releasing the protons from the structure of acidic hybrid microgels, these groups of hybrid microgels convert into their anion forms. HDD of increases owing to electrostatic repulsion between like-charged components within the microgel structure. For example, Ashraf *et al.*[79] have synthesized Ag nanoparticles encapsulated poly(*N*-isopropylmethacrylamide-methacrylic acid) Ag–P(NIMA-MAcA) hybrid microgels. They studied the pH effects on both microgels and hybrid microgels by varying the pH from 2 to 12. Initially the HDD of both systems (microgels and hybrid microgels) did not increase from 2 to 4 but after this pH value, the HDD of hybrid microgels starts to increase rapidly. The pK_a value of methacrylic acid is 4.7. After increasing the pH of medium from 4.7, the carboxylic groups start to convert into carboxylate ions. Due to this conversion, electrostatic repulsion takes place, and the HDD increases. At pH 8, all the carboxylic groups are converted into carboxylate ions and hence maximum repulsion takes place. Therefore, maximum hydrodynamic diameter was obtained at this value. Haleem *et al.*[77] have synthesized Ag NPs decorated in poly(*N*-isopropylacrylamide-2-acrylamido-2-methylpropane-sulfonic acid) P(NIA-AMSA) microgels. They also reported similar effect of pH on the value of hydrodynamic diameter of hybrid microgels due to presence of $-SO_3H$ groups in hybrid microgels.

Hybrid microgels of this kind are highly effective for adsorbents and catalytic reduction of cationic pollutants. In alkaline conditions, these hybrid microgels transform their structure into anionic forms, and in this state, they exhibit the highest attraction to cationic species. As a result, the maximum quantity of cationic pollutants can be reached on the surface of microgels and Ag NPs. However, these systems are less effective for anionic pollutants in such conditions due to electrostatic repulsion.

5.1.2.2. Basic microgels. Such types of hybrid microgels have amino ($-NH_2$) groups in their structures. These amino groups can accept protons from the surrounding medium, transforming their structures into cationic forms. Such hybrid microgels can accept protons are referred to as "basic hybrid microgels". This conversion leads to strong electrostatic repulsion among the structure of hybrid microgels. Therefore, hybrid microgels convert themself into a swelling state. In simple words, these hybrid microgels are in swelling state in acidic conditions and undergo deswelling in basic conditions. Reddy *et al.*[80] have synthesized Ag nanoparticles loaded chitosan/poly(dimethylaminoethylmethacrylate-hydroxyethylacrylate) Ag–CS–P(DMAEMA-HEA) hybrid microgels. They examined the loading and releasing effect on drug at pH 1.2 and 7.4. Maximum drug released pH 7.4 and minimum at 1.2. At pH 1.2, the amino ($-NH_2$) groups of hybrid microgels are converted into cationic forms. Therefore, electrostatic repulsion occurs,

resulting in an increase in hydrodynamic diameter. Therefore, maximum loading and minimum releasing effect was observed at this pH value. But at high pH (pH = 7.4), the amino ($-NH_2$) groups are present in neutral form. Therefore, the value of hydrodynamic diameter decreases in basic medium. Therefore, maximum releasing and minimum loading of drug was observed.

Such hybrid microgels carry positive charges in an acidic environment, making them highly effective adsorbents and catalysts for anionic pollutants under such conditions. This efficiency of hybrid microgels is due to electrostatic interaction between oppositely charged species. Additionally, these microgels are in a swollen state in acidic conditions, which further enhances their suitability as catalyst and adsorbents. However, in these conditions, they exhibit limited adsorption and catalytic capabilities for cationic pollutants due to electrostatic repulsion.

5.1.2.3. Both acidic and basic groups containing hybrid microgels. In such hybrid systems have both acidic (–COOH or $-SO_3H$) and basic (NH_2) groups in their structure. Such type of hybrid microgels are present in cationic form at low pH and anionic form in high pH value. At low pH value, the amino groups are present in protonated form due to basic nature and therefore, electrostatic repulsion takes place. On the other hand, the both acidic –COOH groups and ammonium ions donate their protons. The ammonium ions transfer from positive charged to neutral and –COOH groups from neutral to anionic forms. Due to this conversion, electrostatic repulsion occurs due to the presence of anionic moieties in the structure of hybrid microgels. In these both conditions, the swelling behavior is not prominent due to decreasing the effect of one species in both acidic (–COOH) and basic (NH_2) conditions. Cao *et al.*[81] have synthesized the Ag nanoparticles decorated microgels and these hybrid systems have both $-NH_2$ and –COOH groups in their structure. They studied their different physical parameters such as hardness, elasticity, and deformation. They did not study their optical property.

In the literature, very rarely data are reported on such systems due to their less feasibility towards different reaction such as catalysis and adsorption. This is due to the presence of both acidic and basic groups which oppose the effect of each other. More study is required in these systems for clear identification about their catalytic, adsorption, and optical applications.

5.1.3. Ionic strength. The concentration of ions also has a notable impact on the swelling and deswelling behavior of hybrid microgels. Within the structure of hybrid microgels, there are polar components that generate partial charges or complete positive and negative charges after accepting or donating the protons respectively. These polar and ionic components exhibit affinities for both cations and anions according to their structures. As a result, these regions can be drawn closer to each other through electrostatic attraction when they carry opposite charges, or they can move away from each other due to electrostatic repulsion when they have the same charge within the structure of hybrid microgels. Consequently, the hydrodynamic diameter of the microgels can be influenced by the presence of ionic species. Additionally, charged microgels are strongly affected by the introduction of salts, owing to ion–ion interactions. Oppositely charged ions are attracted to each other due to these ion–ion interactions, while ions with the same charge strongly repel each other. Consequently, the addition of ions of salts in the hybrid microgel dispersion significantly changes the hydrodynamic diameter of the hybrid microgels. The interactions between ionic species are more powerful than those involving partial charges. Therefore, the structure of charged hybrid microgels is profoundly impacted by the addition of salts. Ashraf *et al.*[79] have synthesized Ag NPs loaded poly(*N*-isopropylmethacrylamide-*co*-methacrylic acid) Ag–P(NIMA-MAcA) hybrid microgels. They examined the effect of Na^+ ions by varying the concentration of NaOH. The hydrodynamic diameter of hybrid microgels starts to decrease after pH 8 to 12. In this addition, the content of Na^+ ions increase which strongly interact with the carboxylate ions. Due to this ion–ion interaction, the carboxylation components come close to each other. Therefore, HDD of hybrid systems starts to decrease.

The existence of ionic salts decreases both the mobility and the HDD of microgels. Consequently, the presence of ionic salts leads to a reduction in the adsorption and catalytic efficiency of hybrid microgels. Additionally, it also decreases the thermos-responsive behavior of hybrid microgels, primarily because of strong interactions with metal cations.

5.2. Optical properties of Ag-based hybrid hybrids

The identification of microgel formation is not confirmed by UV-Visible spectrophotometer while the formation of Ag nanoparticles can easily be due to optically active metal nanoparticles such as Ag nanoparticles. Ag nanoparticles in microgels exhibit plasmonic properties. Ag nanoparticles show distinctive bands in the UV-Vis/near-infrared spectrum, depending on the shape and size of Ag NPs. The wavelength (at which the absorbance peak is obtained) is called surface-plasmon-resonance (λ_{SPR}). The UV-Visible spectra obtained by the dispersion of Ag nanoparticles incapsulated microgel can provide valuable awareness about the characterization of Ag nanoparticles.[28]

The optical property of Ag nanoparticles helps to monitor the presence of Ag nanoparticles in microgels by UV/Vis spectroscopy. The loading of salt of silver ions into the microgels initially shows no noticeable peaks, suggesting the absence of Ag nanoparticles. But the UV-Visible spectra display peaks in the visible to infrared range upon the introduction of a reducing agent such as $NaBH_4$, indicating the formation of Ag nanoparticles in microgels.[58]

The increasing intensity of the λ_{SPR} peak over time signifies a rising concentration of Ag nanoparticles as the reaction progresses. The observed red shift in λ_{SPR} value during the reduction process indicates the growth of Ag nanoparticles. Precisely tuning the value of λ_{SPR} of Ag nanoparticles present in the microgels is importance for the applications of hybrid systems in diverse fields, specifically in photo-responsive drug delivery. The key factors influencing the adjustment of λ_{SPR} are discussed in the following sections.

The mole ratio of crosslinker to monomers in the feed content of the microgel plays a critical role in controlling the size of pores in the structure of microgels. A higher crosslinker-to-monomer ratio leads to a denser polymeric network of microgels with more crosslinks. A large quantity of small sized Ag nanoparticles can be obtained, when the synthesis of Ag nanoparticles is done within a highly crosslinked microgel system. On the other hand, fewer large-sized Ag nanoparticles are produced in a microgel system with lower crosslinking density with larger pore sizes. Since the λ_{SPR} band depends on the size of the Ag nanoparticles incorporated into the microgel. Therefore, precise control of the crosslinking density allows for achieving the desired position of the λ_{SPR} band of Ag nanoparticles.[29]

The value of λ_{SPR} band for Ag NPs incorporated in thermo-responsive systems is notably influenced by variations in temperature values. In the case of negative-temperature-responsive hybrid microgels, the polymeric network of hybrid microgels contracts at increasing the temperatures after VPTT. In this way, a reduction occurs in the inter-nanoparticle distance which results in an increase in the refractive index around Ag nanoparticles. Consequently, the λ_{SPR} band value increases. Khan *et al.*[41] conducted a study on the impact of temperature on the λ_{SPR} band value of Ag NPs within microgels. They observed that as the temperature increased from 22 °C to 50 °C, the λ_{SPR} band shifted from 429 to 416 nm. This behavior is attributed to the removal of water from the microgel network, which raised the refractive index. Li *et al.*[53] also examined the effect of temperature by varying from 20 °C to 50 °C on hybrid microgels. They observed a red shift in the λ_{SPR} band value.

Solvents are also affected on the λ_{PSR} value of Ag nanoparticles which exist in polymeric systems. The value of refractive index of each solvent is different. The value of λ_{PSR} band of Ag NPs in microgels is obtained at longer wavelengths if the refractive index of solvent is higher than others. On the other hand, the value of λ_{PSR} band is achieved at shorter wavelengths if the refractive index value of solvent is lower than others. Li *et al.*[82] have synthesized Ag based and Ag/Au-based hybrid systems. They investigated the effect of solvents on λ_{PSR} band value. They used acetone, water, tetrahydrofuran, and carbon disulfide medium. Carbon disulfide has the highest refractive index among all. Therefore, the value of λ_{PSR} band is obtained at 467 nm and 600 nm for Ag based and Ag/Au-based hybrid systems respectively. On the other hand, water has the lowest refractive index value. In this solvent, the value λ_{PSR} band is achieved at 446 nm and 578 nm for Ag based and Ag/Au based hybrid microgels respectively.

The content of other metal nanoparticles also effects on the λ_{PSR} band value of Ag nanoparticles. The value of λ_{PSR} band shows blue shift if non surface plasmon resonance active metal nanoparticles are introduced along with the Ag nanoparticles in microgels. And a red shift is achieved of surface plasmon resonance active metal nanoparticles like Au NPs are added along with Ag nanoparticles in microgels. The shifting band peak can show two peaks or single broad peaks of bimetallic nanoparticles. Melinte *et al.*[83] have synthesized Ag based, Au based, and Ag/Au based hybrid microgels. They observed that the λ_{SPR} band value of Ag nanoparticles shifted to the longer wavelength. The value of λ_{SPR} band was found at 419 nm for bare Ag nanoparticles-based hybrid microgels and this value shifted from 419 nm to 437 nm in bimetallic (Ag/Au) nanoparticles-based hybrid microgels. Similar trends were reported through Li *et al.*[82] by increasing the content of Au nanoparticles along with Ag nanoparticles in microgels.

The swelling and deswelling behavior of hybrid systems can be controlled with the help pf pH of the medium. This swelling and deswelling behavior change the environment of Ag nanoparticles which affects the k_{SPR} band value of Ag nanoparticles. Hussain *et al.*[59] have studied the pH effect on k_{SPR} band value. They increased the pH value of medium from 3.1 to 8.4. In this condition, the –COOH groups are converted into carboxylate ions. Due to this conversion, the Ag nanoparticles diffuse to other sieves and then coagulation occurs. Therefore, the k_{SPR} band value increased with increasing the pH of the medium. Similar trends were reported in Ag based acid hybrid microgel by Zahid *et al.*[40] Siddiq *et al.*[37] have synthesized Ag based acidic hybrid microgels. The value of k_{SPR} band shifted from 394 nm to 403 nm when the pH of medium changed from 2 to 10.

Ag nanoparticles are typically synthesized within microgels through the *in situ* precursor salt reduction approach. The size of the resulting nanoparticles depends on the concentration of the precursor and crosslinking density. Consequently, the position of λ_{SPR} can be controlled by adjusting the feed concentration of Ag nanoparticles in microgels. As the concentration of Ag salt increases or decreases the crosslinking density, larger Ag nanoparticles are generated which results to a broader and longer-wavelength shift in the λ_{SPR} band. Moreover, the intensity of the λ_{SPR} band increases with the increased content of Ag nanoparticles. Li *et al.*[53] have synthesized Ag nanoparticles encapsulated microgel systems with various content of Ag salt during synthesis. As the content of Ag salt increases the size of Ag nanoparticles increased. Therefore, the λ_{SPR} band value shifts to longer wavelengths as the content of Ag salt increases during synthesis.

6. Applications of Ag-based hybrid microgels

Ag nanoparticles decorated microgels have different applications in various fields as shown in Fig. 5, which will be elaborated on individually in the following sections.

6.1. Adsorption of pollutants

Hybrid microgels can also be used as adsorbent for adsorption of various pollutants from water. The structure of hybrid microgels have some polar functional groups such as –COOH, –SO_3H, –CONH–, and –NH_2. These groups can make dipole–dipole interaction or ion–dipole interaction or hydrogen bonding with different dyes, metal cation, and other pollutants. Therefore, the pollutants can easily be attached on the surface of hybrid microgels due to these interactions. Pandey *et al.*[84] have synthesized Ag nanoparticles decorated in microgels. They used these hybrid microgels for adsorption of crystal violet dye

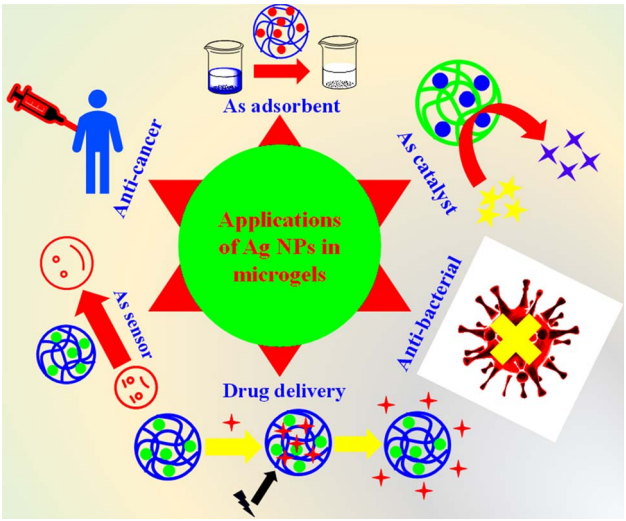

Fig. 5 Applications of Ag NP encapsulated microgels in various fields.

from water. They obtained 99% removal of this dye from water at pH 8. Similarly, Atta *et al.*[85] have synthesized and used the Ag nanoparticles decorated hybrid systems for adsorption of methylene blue dye from water. The percentage removal of dye was increased with increasing the pH of the medium. As the pH of the medium increases, the acidic groups release their protons and become in anionic form. These anions have more affinity towards the cationic methylene blue dye. Therefore, the percentage removal of dye increases with increasing the pH of the medium.

6.2. Catalysis

Ag NPs decorated microgels are widely utilized as catalysts for a range of organic reactions. The combined property of both smart microgels and Ag NPs make the hybrid microgels excellent for catalytic reactions. The Ag-based hybrid systems offer several advantages over conventional catalytic systems.

(1) The strong acceptor–donor interactions between Ag NPs and the different functionalities of polymer microgels render the Ag NPs highly stable within the crosslinked polymeric network. They remain securely within the network, even during catalytic processes.[86]

(2) The open structure of the polymeric network facilitates the easy access of reactant molecules to the surface of Ag NPs, enabling efficient catalysis.

(3) The catalytic activity of hybrid systems can be modulated by altering the environmental conditions such as pH[87] and temperature[88] of medium.

(4) Hybrid systems can be easily detached after converting reactants into products, simply through centrifugation or by employing a magnet in the case of magnetic hybrid systems.

(5) The structure of polymer is typically chemically inert and does not actively participate in the catalytic conversions.[55]

(6) In certain instances where chemical reactions are catalyzed by Ag-based systems, the polymeric network provides a supportive environment that enhances the approaches of reactants from the bulk to the Ag surface, thereby contributing to rate enhancement.

The subsequent sections provide an exploration of the organic reactions catalyzed by Ag NPs decorated in microgels.

6.2.1. Reduction of nitroarenes. Ag NPs decorated microgels find extensive application as catalysts for the reduction of nitroarenes with $NaBH_4$ in water. The catalytic reduction of nitroarenes using Ag NPs decorated microgels primarily comprises four sequential steps. Initially, the hydrogen from $NaBH_4$ and nitroarene are adsorbed onto the Ag NPs surface. Subsequently, the interactions are generated between the adsorbed materials in the second step. In the third step, nitroarenes are transformed into amino-arenes on Ag NPs surface. Finally, the products (amino-arenes) are detached from the surface of Ag NPs in the fourth step. During this conversion, there are two possibilities of reaction mechanism as shown in Fig. 6. The reaction which occurred very fast followed route-II for reaction and those which take some time for completion followed route-I.

The catalytic reduction of 4NiP into 4-aminophenol (4AmP) is widely employed as a model reaction to assess the catalytic performance of Ag NPs decorated systems. The choice of this model reaction is motivated by the toxicity of 4NiP, which is transformed into the relatively less toxic 4AmP. 4AmP is commonly used in the preparation of numerous pigments and dyes, and the reduction of 4NiP can be easily monitored using a UV/Vis spectrophotometry. When 4NiP begins to undergo conversion into 4AmP, there is a decrease in the absorbance of the peak at 400 nm, while another peak starts to emerge around 300 nm. The decline in the absorbance at 400 nm over time serves as a means to monitor the advancement of the reaction. As the entire quantity of 4NiP is transformed into 4AmP, the 400 nm peak vanishes, leaving a single peak at approximately 300 nm in a slightly basic medium. Mao *et al.*[89] have synthesized Ag NPs decorated microgels and employed for conversion of 4NiP into 4AmP. Similar results are obtained in the decline of absorbance (at 400 nm) and appearance at 300 nm. The effect of temperature and pH is also studied in this conversion. Similar trend has also been reported by Sarkar *et al.*[90] and Feng *et al.*[91] for the reduction of 4NiP in the presence of Ag NPs decorated systems.

Several factors influence the catalytic reduction performance of Ag NPs decorated microgels for nitroarenes. These factors are given below.

The quantity of Ag NPs in crosslinked network of polymer is a crucial factor that significantly impacts the reduction rate of nitroarenes as shown in Fig. 7. The catalytic reduction rate of nitroarenes increases with increasing the content of Ag NPs in microgels. Li *et al.*[53] have synthesized Ag nanoparticles in microgels. They found that the content of Ag NPs in microgel systems was higher, leading to better catalytic performance in those hybrid systems. As the content of Ag nanoparticles is greater in hybrid microgels then the surface area of Ag NPs also increases. Therefore, the catalytic efficiency of hybrid microgels increases.

Temperature also has an impact on the rate of nitroarene reduction catalyzed by Ag NPs containing hybrid systems as

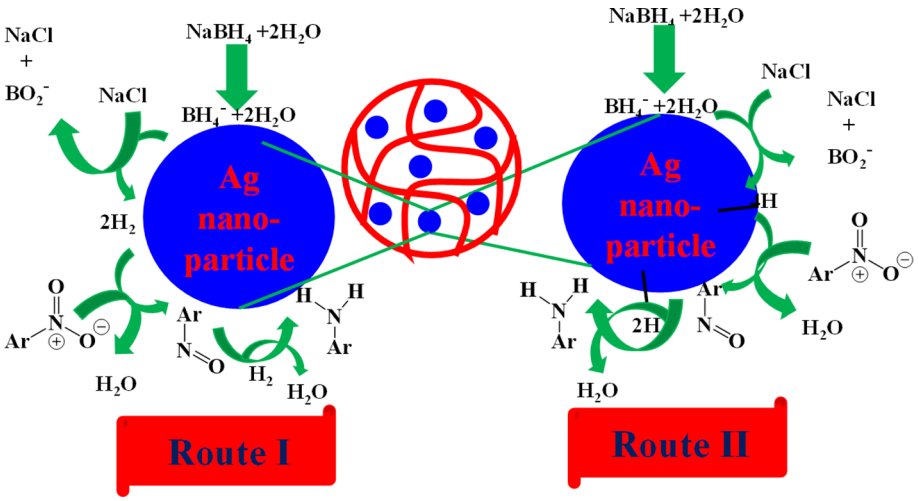

Fig. 6 Proposed catalytic reduction mechanism of 4NiP.

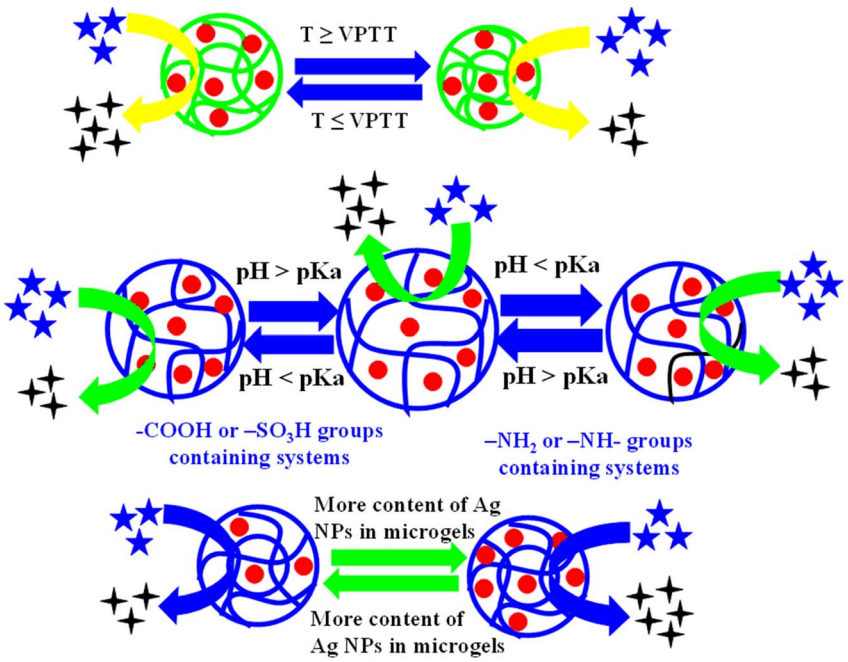

Fig. 7 Different catalytic reduction reaction affecting factors (reproduced from ref. 11 with permission from Elsevier, copyright 2023).[11]

shown in Fig. 7. However, the temperature dependence of the reaction rate deviates from the typical Arrhenius behavior. The value of HDD of hybrid microgels decreases as the temperature of the medium rises. The value of temperature, at which the value of HDD of hybrid microgels rapidly decreases, is known as the Volume Phase Transition Temperature (VPTT). At temperatures below VPTT, reactants can efficiently access the surface of Ag NPs with significant diffusion, leading to rapid conversion into products. However, as the temperature exceeds VPTT, the rate of the catalytic reaction decreases due to the shrinkage of hybrid microgels and the reduction in HDD, making it challenging for reactants to reach the surface of catalyst.

The application of the Arrhenius equation offers a quantitative approach to analyze the impact of temperature on the reaction rate. It has been studied that the natural logarithm of k_{obs} is not a linear function of $1/T$ within a temperature range that encompasses the Volume Phase Transition Temperature (VPTT). The k_{obs} value decreases with increasing temperature, reaching a minimum at VPTT, and subsequently starts to increase beyond VPTT. This complex temperature-dependent behavior has been investigated by Shah *et al.*[92] and Naseem *et al.*[93] in the context of the reduction of 4NiP catalyzed by Ag NPs decorated microgels.

The catalytic performance of Ag-based hybrid systems can also be controlled by adjusting the pH of the medium as shown in Fig. 7. This pH-dependent effect is attributed to the existence of acidic (–COOH, $–SO_3H$) and basic (NH_2) groups in the structure of hybrid systems. The pH impact on these acidic and

basic groups is opposite for the reason that one group can release a proton due to its acidic property, while the other group accepts a proton due to its basic property. Hybrid systems, which contain –COOH or $–SO_3H$ groups, exhibit swelling on increasing the pH. When the pH $\geq$ pK_a, then all $–SO_3H$ or –COOH groups are changed into $–SO_3^-$ or $–COO^-$ groups respectively. These anionic groups repel each other because of electrostatic repulsion, leading to an increase in the HDD of the microgel particles. In the swollen state of hybrid microgels, a large quantity of reactants can easily access the Ag NPs surface, resulting in the conversion of a significant number of reactants into products with a high observed rate constant. On the other hand, if pH $\leq$ pK_a, the hybrid systems are in a deswelling state, and only a few numbers of reactants can come to the Ag NPs surface, resulting to the formation of a few numbers of products. Rahman *et al.*[50] investigated the impact of pH on the catalytic activity of hybrid systems. They observed that the value of k_{obs} at pH 2.01 was 0.149 min^{-1}, while at pH 10.0, it increased to 0.350 min^{-1}. Haleem *et al.*[77] also reported similar trend for catalytic reduction of nitroarenes at various pH values. They used $–SO_3H$ groups containing hybrid microgels.

When hybrid systems contain $–NH_2$ groups within their structure, the catalytic activity of these hybrid systems can be modulated by adjusting the pH of medium as shown in Fig. 7. The $–NH_2$ groups are present in protonated form at low pH level, leading to electrostatic repulsion by reason of cationic forms present in the structure. Consequently, the HDD of hybrid systems is high at lower pH values and decreases as the pH is increased. Such systems are not suitable for catalytic reduction in this duration.

The introduction of Ag NPs in microgels loaded with other metal nanoparticles has a significant impact on the catalytic efficiency of hybrid systems for reduction of nitroarenes. The catalytic efficiency of hybrid systems can be enhanced either by incorporating Ag NPs into other metal NPs containing systems or by introducing other metal NPs into Ag NPs containing systems. When NPs of one metal are introduced into hybrid systems that already contain NPs of another metal, an interface is formed between the other metal NPs and the Ag NPs, leading to an increase in catalytic efficiency. The work function values of other metal NPs and Ag NPs play a key role in the generation of a depletion region. Electrons flow from the side with a lower work function to the side with a higher work function, leading to interactions between electron-rich sodium borohydride and electron-deficient reactants such as 4NiP and *vice versa*. This interaction allows a large quantity of reactant to access the surface of the nanoparticles, resulting in rapid reduction.[60,61,83] Li *et al.*[82] conducted the synthesis of bimetallic hybrid systems by incorporating Au NPs with varying contents into microgels that already contained Ag nanoparticles. They investigated the catalytic performance of each of these hybrid microgels. The findings revealed that the value of k_{obs} increased as the content of Au NPs in the hybrid systems was augmented, representing the catalytic rate for the reduction of 4NiP. In a similar manner, Velpula *et al.*[94] also reported an enhancement in the catalytic efficiency of Ag-based systems by introducing Au or Pd nanoparticles into hybrid systems.

The $NaBH_4$ concentration also has an impact on the reduction rate of nitroarene. When the quantity of $NaBH_4$ is increased, the value of k_{obs} also increases resulting in a shorter reaction time. At higher concentrations of $NaBH_4$, a greater amount of the reagent molecules is adsorbed on the surface of the Ag nanoparticles and subsequently released in the form of the greater product molecules. Mustafa *et al.*[42] conducted a study on the catalytic performance of Ag NPs containing microgels at various $NaBH_4$ concentrations. The reaction rate increases with higher concentrations of $NaBH_4$.

The k_{obs} value is also dependent on the number of nitro groups which are directly bonded with benzene ring. As a result, the k_{obs} value of tri-nitroarene reduction is lower than that of mono-nitroarene under similar conditions. Arenes containing mono-nitro groups are reduced more rapidly than nitroarenes with more than one nitro group. Raza *et al.*[95] performed reduction reactions on 4NiP, and 2,6-dinitrophenol (2,6-DNiP) and calculated k_{obs} values for each reaction. The k_{obs} value was found greater for 4NiP than 2,6-DNiP.

6.2.2. Dyes reduction/degradation. Dyes are significant water pollutants, and their elimination from water sources is a worthy environmental task. The catalytic degradation/reduction of toxic dyes from water has emerged as an effective method for eliminating such harmful substances from aqueous environments. Ag NPs containing microgel systems have been frequently employed for the catalytic degradation/reduction of dyes. During the reduction of azo dyes, the azo dye and hydrogen from sodium borohydride come on the surface and both reactants adsorbed on the surface of metal NPs. These azo groups of azo dyes are converted into two amino groups in the form of product. Then the products are detached from the surface of metal nanoparticles. The proposed mechanism for reduction of azo dyes is shown in Fig. 8.

Naseem *et al.*[96] have synthesized the P(StR)@P(NIMA-AcA) core–shell microgel systems and then Ag NPs were fabricated in shell region of these systems. The synthesized systems were employed for reduction of CoR dye from water. Shah *et al.*[92] have also synthesized a microgel system. Both Ag and Au NPs were separately introduced in the synthesized microgel systems to make Ag containing microgels and Au containing microgel systems. These hybrid microgels were then used for the catalytic reduction/degradation of CoR and MeB from water. Additionally, Shahid *et al.*[34] have synthesized and utilized the Ag nanoparticles-based hybrid microgels for the catalytic reduction of CoR and MeO dyes. The reduction of MeO was found to be fast as compared to the reduction of CoR dye. This is because only one azo group is present in MeO dye while two in CoR. Therefore, the reduction of CoR dye takes more time than MeO. The reduction of organic dyes is faster as compared to nitroarenes. Generally, the dyes have charge in their structure and string electron withdrawing groups. Due to these factors, dyes rapidly reach the surface of the Ag nanoparticles which provides the electron from reducing agent like $NaBH_4$. On the other hand, mostly nitroarenes have no charge and no electron withdrawing groups in their structures. Therefore, their affinity towards electrons is less than organic dyes. Therefore, the

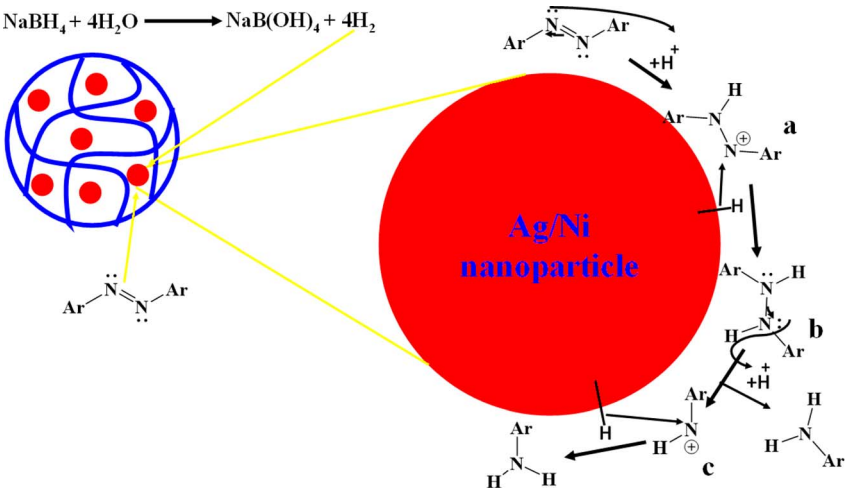

Fig. 8 Most probable catalytic reduction mechanism for azo dyes.[55]

catalytic reduction reactions of nitroarenes are slower than organic dyes. Similar trends were observed by Parida *et al.*[97]

6.2.3. Reduction of metal ions. Ag nanoparticles encapsulated microgels can also be used for catalytic reduction of toxic metal cations such as Cr^{6+} ions. Chromium metal exists in two oxidation states: Cr^{6+} and Cr^{3+} ions. Both ions are commonly involved in biological processes and are essential for insulin function. Cr^{6+} ions containing compounds are generally more reactive and toxic than their trivalent compounds. Cr^{6+} ions are frequently associated with environmental pollution and health concerns due to their carcinogenic properties. The stark differences in stability and reactivity between Cr^{3+} and Cr^{6+} ions underscore the importance of understanding their distinct roles in various contexts. Therefore, it is very important to convert the Cr^{6+} ions into Cr^{3+} ions. Hussain *et al.*[59] have synthesized the core–shell microgel system and then Ag NPs were introduced in the shell region of this core–shell system. They used these hybrid systems to reduce Cr^{6+} ions into Cr^{3+} ions in the presence of formic acid and Ag nanoparticles encapsulated core–shell microgel systems. This study also included an examination of the stability of Ag NPs in core–shell system across a wide range of pH and temperature conditions. Raza *et al.*[95] have also synthesized bimetallic (Ag/Ti) nanoparticles encapsulated microgel systems and then employed for reduction of Cr^{6+} ions. They also reduced different other compounds along with Cr^{6+} ions from water.

6.3. Application of hybrid microgels for sensing

Ag NPs encapsulated microgels have the properties of sensing. This property of hybrid microgels is very important for awareness related to other species. One most important property of Ag nanoparticles encapsulated microgels is the detection of humidity from environment. The hybrid microgels absorb the water molecules from the environment due to presence of polar moieties in their structure and their swelling behavior. Li *et al.*[98] have synthesized Ag NPs containing hybrid microgels and used these for detection of humidity. Hybrid microgels can also be used for detection of H_2O_2. During this detection the absorption band of hybrid microgels changes resulting in a change in color. In this way, the detection of H_2O_2 can easily be monitored by naked eye. Shu *et al.*[52] have synthesized Ag nanoparticles loaded poly(*N*-isopropylacrylamide-acrylic acid) Ag–P(NIA-AcA) hybrid microgels. They employed these hybrid microgels for detection of H_2O_2. They observed a red shift in the reflectance peak after the addition of H_2O_2 in the dispersion of hybrid microgels. This dual position of signal of peaks is obtained due to the oxidative breakdown of Ag nanoparticles, increases in reflection of lights by expansion of hybrid microgels. George *et al.*[67] have also synthesized the Ag nanoparticles containing chitosan–poly(-acrylic acid) CS–P(AcA) microgels. They applied these hybrid systems for sensing H_2O_2. They also detect H_2O_2 from samples of real milk.

6.4. Applications in biological field

Ag nanoparticles-based hybrid microgels are used in different types of biological fields. Let us now discuss them one by one.

6.4.1. Use of Ag NPs decorated microgels for drug delivery. Smart microgels containing Ag nanoparticles find extensive application as drug delivery systems due to their ability to respond to changes in temperature, pH, and electromagnetic radiation. These parameters are adjusted to maximum loading and releasing the drug from hybrid microgels. These factors control the swelling and deswelling behavior of microgels with stimuli. Generally, the drug is loaded at low temperature (swelling) and released by increasing the temperature (deswelling). During this conversion of swelling state to deswelling state, the drug comes out from the hybrid microgels along with water molecules. But the releasing of this loaded drug is not hundred percent. Some amount of loaded drug remains into the crosslinked network of microgels due to large interactions (present more inner side of microgels). The drug which is present on the surface or near outer surface easily come out during deswelling, but the more inner drug cannot come out. On the other hand, more drug is released from the swelling state of microgels than deswelling state during centrifugation due to easy diffusion rate in swelling state than deswelling state.

Gholamali *et al.*[43] have synthesized pH responsive hybrid microgels and used these hybrid microgels for releasing of drug at various pH of the medium. The releasing effect is monitored due to deswelling behavior of hybrid microgels. Batool *et al.*[99] have also synthesized Ag NPs based hybrid microgels and used for drug delivery. They applied ciprofloxacin for loading and releasing from hybrid microgels.

6.4.2. Antibacterial activities. To assess the biocompatibility of the developed composites, outstanding compatibility has been reported in various articles in literature.[41,100,101] This biocompatibility is maintained due to the stability of Ag nanoparticles in microgels. Silver nanoparticles (Ag NPs) possess excellent antibacterial properties due to their capability to release Ag^+ ions into an aqueous solution through the porous microgel network, outperforming bulk silver. Remarkably, Ag NPs exhibit antibacterial activities without releasing toxic agents.[102] Furthermore, they can bind to electron-donating groups like thiol, carboxylate, and phosphate groups present in DNA, leading to the disruption of normal cellular processes in bacterial cells.[103] Consequently, they serve as highly effective bactericidal agents against a range of bacteria, including *Escherichia coli*,[104] *Staphylococcus aureus*,[104,105] *Candida albicans*,[106] and *Pseudomonas aeruginosa*.[107]

El-Aassar *et al.*[108] have synthesized Ag nanoparticles based crosslinked polymer microgels. These hybrid microgels were employed against human pathogenic bacteria. The hybrid microgels showed excellent results against these bacteria. Salama *et al.*[109] have also synthesized Ag nanoparticles-based hybrid microgels. They obtained 15% to 26% killing of different types of bacteria. The Ag nanoparticles decorated microgel systems are more suitable for antibacterial due to their high efficiency.[110]

6.4.3. Anti-cancer. Hybrid microgels based on Ag nanoparticles have shown promise in the field of cancer treatment, offering a contribution from their organic portion of hybrid microgels. The anti-cancer drug is loaded in hybrid microgels and released by applying radiation at the target place. The anti-cancer drug is released due to deswelling behavior of hybrid microgels. Capanema *et al.*[111] have synthesized Ag based hybrid systems. They used doxorubicin for loading and cancer treatment. The efficiency of crosslinked polymer alone is very small. The efficiency rapidly increases by loading doxorubicin in Ag nanoparticles loaded crosslinked polymer systems. This efficiency is due to both Ag nanoparticles and drug. The toxicity of doxorubicin also decreased in both crosslinked polymer and hybrid systems.

7. Conclusion and future directions

We have provided an overview of recent advancements in the synthesis, categorization, and characteristics of smart polymer microgels containing silver nanoparticles. This review briefly outlines the characterization techniques employed for assessing microgels fabricated with silver nanoparticles. The stimuli responsive behavior, optical study, and various applications of Ag nanoparticles encapsulated microgel systems in the fields of biomedical science, catalysis, and environmental science have been explained critically in this review article. The fabrication of silver nanoparticles within smart polymer microgels holds significant importance due to the interesting optical properties of silver nanoparticles and the responsive behavior of the microgels.

Identification of biomolecules is a major challenge now-a-day. This challenge can be achieved by using Ag-based hybrid systems. These systems are used as optical biosensors in this regard. But this behavior is limited to a specific content of Ag nanoparticles in microgels below which these systems are not applicable. Ag nanoparticles encapsulated can be considered an ideal platform for catalytic applications. The catalytic performance of this hybrid system can be adjusted through external factors such as temperature, pH, and ionic strength. The interest of researchers has been steadily growing in this field, as evidenced by this review. The catalytic performance of these systems can be controlled by controlling the condition of the medium. In this way, they can cover all types of pollutants (cationic, ionic, and neutral) and reduce the selective reducing time. This review article outlines recent advances in the fabrication of Ag nanoparticles in smart microgels, which is expected to pave the way for further research in this domain. Additionally, it anticipates potential areas for future investigation. From a biological perspective, it is priority that these hybrid microgels are non-carcinogenic, non-toxic, and exceptionally stable to prevent any adverse effects within the body. The controlled or complete prevention of silver nanoparticles leaching from the crosslinked polymeric network of microgel is a crucial aspect that has not yet received adequate attention in the literature. Consequently, drug delivery systems must be designed to function effectively under physiological pH and temperature conditions.

These Ag nanoparticle-based hybrid microgels serve as effective anti-bacterial and drug carriers, with some from these drug delivery systems based on the treatment for tumor and cancer. However, a significant portion of the drug delivery and anti-bacterial systems reported in the past eight years relies on *N*-isopropylacrylamide which is a thermo-responsive monomer that is not readily biodegradable. In forthcoming research, it could be advantageous to consider substituting this with a biodegradable monomer like 4-vinylcaprolactam.

Furthermore, Ag-based polymer systems have found utility as catalysts in specific organic reactions. The catalytic potential of these hybrid systems in several organic transformations warrants further exploration in future considerations. Notably, the catalytic reduction/degradation of pollutants (nitroarenes and dyes) with Ag NPs containing microgels has been a focal point of interest over the last eight years, although most studies have concentrated on catalytic reduction of a model reaction, specifically for 4NiP. To make this hybrid system more practical, it is essential to investigate a broader range of substrates for catalytic transformation in future research.

Abbreviations

AcA	Acrylic acid
NIMA	*N*-Isopropylmethacrylamide

NIA	*N*-Isopropylacrylamide
NPs	Nanoparticles
P(NIA)	Poly(*N*-isopropylacrylamide)
EtI	Ethyleneimine
MeB	Methylene blue
CoR	Congo red
4NiP	4-Nitrophenol
DLS	Dynamic light scattering
SoDS	Sodium dodecyl sulfate
MeO	Methyl orange
EDX	Energy dispersive X-rays
HDD	Hydrodynamic diameter
FTIR	Fourier transformed infrared spectroscopy
FRPPM	Free radical precipitation polymerization method
HRTEM	High resolution transmission electron microscopy
MAcA	Methacrylic acid
UCST	Upper critical solution temperature
HEM	2-Hydroxyethylmethacrylate
CS	Chitosan
MeBA	*N*,*N*′-Methylene-bisacrylamide
AmPS	Ammonium persulfate
BrB	Brilliant blue
AcAm	Acrylamide
AMSA	2-Acrylamido-2-methylpropane sulfonic acid
AlAm	Allylamine
SEM	Scanning electron microscopy
StR	Styrene
SPR	Surface plasmon resonance
CMCS	Carboxymethyl chitosan
TGA	Thermo gravimetric analysis
DMAEMA	Dimethylaminoethylmethacrylate
CL	Cellulose
UV-Vis	UV/Visible spectroscopy
HLNA	Hyaluronic acid
VPTT	Volume phase transition temperature
P(EtI)	Poly(ethyleneimine)
XPS	X-ray photoelectron spectroscopy
NNPA	*N*-*n*-Propylacrylamide
XRD	X-ray diffraction
HEA	Hydroxyethylacrylate
ICP-AES	Inductively coupled plasma-atomic emission spectroscopy
FRPPM	Free radical precipitation polymerization
RAmB	Rhodamine B

Data availability

Data will be provided on request.

Conflicts of interest

There is no conflict of interest.

Acknowledgements

Muhammad Arif is thankful to University of Management and Technology, Lahore-54770, Pakistan.

References

1 X. Liu, Q. Zhang, L. Duan and G. Gao, *Adv. Funct. Mater.*, 2019, **29**, 1900450.
2 A. K. Nayak and B. Das, *Polym. Gels*, 2018, 3–27.
3 C. Echeverria, S. N. Fernandes, M. H. Godinho, J. P. Borges and P. I. P. Soares, *Gels*, 2018, **4**, 54.
4 N. Majstorović and S. Agarwal, *ACS Appl. Polym. Mater.*, 2022, **4**, 5996–6005.
5 Y. Kittel, A. J. C. Kuehne and L. De Laporte, *Adv. Healthcare Mater.*, 2022, **11**, 2101989.
6 J. Wei, H. Yu, H. Liu, C. Du, Z. Zhou, Q. Huang and X. Yao, *J. Mater. Sci.*, 2018, **53**, 12056–12064.
7 C. S. A. de Lima, T. S. Balogh, J. P. R. O. Varca, G. H. C. Varca, A. B. Lugão, L. A. Camacho-Cruz, E. Bucio and S. S. Kadlubowski, *Pharmaceutics*, 2020, **12**, 970.
8 M. Karg, A. Pich, T. Hellweg, T. Hoare, L. A. Lyon, J. J. Crassous, D. Suzuki, R. A. Gumerov, S. Schneider, I. I. Potemkin and W. Richtering, *Langmuir*, 2019, **35**, 6231–6255.
9 M. Arif, Z. H. Farooqi, A. Irfan and R. Begum, *J. Mol. Liq.*, 2021, **336**, 116270.
10 M. Arif, H. Raza and S. M. Haroon, *JOM*, 2023, **75**, 5217–5234.
11 M. Arif, *Mater. Today Commun.*, 2023, **36**, 106580.
12 M. Dirksen, C. Dargel, L. Meier, T. Brändel and T. Hellweg, *Colloid Polym. Sci.*, 2020, **298**, 505–518.
13 C. C. Cutright, J. L. Harris, S. Ramesh, S. A. Khan, J. Genzer and S. Menegatti, *Adv. Funct. Mater.*, 2021, **31**, 2104164.
14 Y. A. Rozhkova, D. A. Burin, S. V. Galkin and H. Yang, *Gels*, 2022, **8**, 112.
15 Y. Wang, L. Guo, S. Dong, J. Cui and J. Hao, *Adv. Colloid Interface Sci.*, 2019, **266**, 1–20.
16 F. Li, D. Lyu, S. Liu, W. Guo, F. Y. Li, D. Y. Lyu, S. Liu and W. W. Guo, *Adv. Mater.*, 2020, **32**, 1806538.
17 M. Arif, *J. Environ. Chem. Eng.*, 2023, **11**, 109270.
18 M. Arif, M. Shahid, A. Irfan, J. Nisar, X. Wang, N. Batool, M. Ali, Z. H. Farooqi and R. Begum, *Z. Phys. Chem.*, 2022, **236**, 1219–1241.
19 M. Arif, M. Shahid, A. Irfan, J. Nisar, W. Wu, Z. H. Farooqi and R. Begum, *RSC Adv.*, 2022, **12**, 5105–5117.
20 G. Agrawal and R. Agrawal, *Polymers*, 2018, **10**, 418.
21 R. A. Gumerov, E. Gau, W. Xu, A. Melle, S. A. Filippov, A. S. Sorokina, N. A. Wolter, A. Pich and I. I. Potemkin, *J. Colloid Interface Sci.*, 2020, **564**, 344–356.
22 P. Saha, M. Santi, M. Frenken, A. R. Palanisamy, R. Ganguly, N. K. Singha and A. Pich, *ACS Macro Lett.*, 2020, **9**, 895–901.
23 M. Annegarn, M. Dirksen and T. Hellweg, *Polymers*, 2021, **13**, 827.
24 A. D. Drozdov and J. d. C. Christiansen, *Polymer*, 2021, **221**, 123637.
25 M. Arif, *JOM*, 2024, **76**, 1203–1222.
26 M. Arif, H. Raza, S. M. Haroon, K. Naseem, H. Majeed, F. Tahir, U. Fatima, S. M. Ibrahim and S. Ul Mahmood, *J. Mol. Liq.*, 2023, **392**, 123541.
27 M. Arif, *Z. Phys. Chem.*, 2023, **237**, 809–843.

28 R. Begum, Z. H. Farooqi, K. Naseem, F. Ali, M. Batool, J. Xiao and A. Irfan, *Crit. Rev. Anal. Chem.*, 2018, **48**, 503–516.
29 T. Brändel, V. Sabadasch, Y. Hannappel and T. Hellweg, *ACS Omega*, 2019, **4**, 4636–4649.
30 M. Arif, *Polymers*, 2023, **15**, 3600.
31 X. Lv, A. Lv, S. Tian, T. Xie and S. Sun, *Eur. Polym. J.*, 2023, **182**, 111713.
32 R. Begum, Z. H. Farooqi, A. H. Aboo, E. Ahmed, A. Sharif and J. Xiao, *J. Hazard. Mater.*, 2019, **377**, 399–408.
33 P. Bhol and P. S. Mohanty, *J. Phys.: Condens. Matter*, 2020, **33**, 084002.
34 M. Shahid, Z. H. Farooqi, R. Begum, M. Arif, M. Azam, A. Irfan and U. Farooq, *Z. Phys. Chem.*, 2022, **236**, 87–105.
35 M. Arif, F. Tahir, U. Fatima, R. Begum, Z. H. Farooqi, M. Shahid, T. Ahmad, M. Faizan, K. Naseem and Z. Ali, *Mater. Today Commun.*, 2022, 104700.
36 M. Arif, *J. Mol. Liq.*, 2024, **403**, 124869.
37 M. Siddiq, K. Bakhat and M. Ajmal, *Pure Appl. Chem.*, 2020, **92**, 445–459.
38 L. A. Shah, *J. Mol. Liq.*, 2019, **288**, 111045.
39 L. Liu, D. Li and W. Deng, *Biosens. Bioelectron.*, 2021, **180**, 113138.
40 S. Zahid, A. K. Alzahrani, N. Kizilbash, J. Ambreen, M. Ajmal, Z. H. Farooqi and M. Siddiq, *RSC Adv.*, 2022, **12**, 33215–33228.
41 A. Khan, T. H. Khan, A. M. El-Toni, A. Aldalbahi, J. Alam and T. Ahamad, *Mater. Lett.*, 2019, **235**, 197–201.
42 G. Mustafa, P. Ghosh Roy, S. Zhou, A. Irfan, A. R. Chaudhry, R. Begum and Z. H. Farooqi, *J. Mol. Liq.*, 2023, **385**, 122397.
43 I. Gholamali, M. Asnaashariisfahani and E. Alipour, *Regener. Eng. Transl. Med.*, 2020, **6**, 138–153.
44 R. Begum, K. Naseem and Z. H. Farooqi, *J. Sol-Gel Sci. Technol.*, 2016, **77**, 497–515.
45 A. Ahmad, P. G. Roy, S. Zhou, A. Irfan, F. Kanwal, R. Begum and Z. H. Farooqi, *Int. J. Biol. Macromol.*, 2023, **240**, 124401.
46 J. Ambreen, F. F. Al-Harbi, H. Sakhawat, M. Ajmal, H. Naeem, Z. H. Farooqi, N. Batool and M. Siddiq, *J. Mol. Liq.*, 2022, **355**, 118931.
47 Z. H. Farooqi, K. Naseem, A. Ijaz and R. Begum, *J. Polym. Eng.*, 2016, **36**, 87–96.
48 R. Begum, K. Naseem, E. Ahmed, A. Sharif and Z. H. Farooqi, *Colloids Surf., A*, 2016, **511**, 17–26.
49 Y. Han, X. Wu, X. Zhang, Z. Zhou and C. Lu, *ACS Sustain. Chem. Eng.*, 2016, **4**, 6322–6331.
50 S. Rahman, F. F. Al-Harbi, M. Ajmal, A. Naseem, Z. H. Farooqi and M. Siddiq, *J. Mater. Sci.*, 2022, **57**, 6763–6779.
51 S. Noureen and S. Ashraf, *Chem. Phys. Impact*, 2023, **6**, 100142.
52 T. Shu, Q. Shen, Y. Wan, W. Zhang, L. Su, X. Zhang and M. J. Serpe, *RSC Adv.*, 2018, **8**, 15567–15574.
53 K. Li, X. Chen, Z. Wang, L. Xu, W. Fu, L. Zhao and L. Chen, *Polym. Compos.*, 2017, **38**, 708–718.
54 M. Arif, *J. Mol. Liq.*, 2023, **375**, 121346.
55 M. Arif, *RSC Adv.*, 2023, **13**, 3008–3019.
56 M. Arif, *Eur. Polym. J.*, 2024, **206**, 112803.
57 M. Arif, *J. Mol. Liq.*, 2024, **403**, 124869.
58 K. Naseem, R. Begum, W. Wu, A. Irfan, A. G. Al-Sehemi and Z. H. Farooqi, *J. Cleaner Prod.*, 2019, **211**, 855–864.
59 I. Hussain, F. Ali, M. Shahid, R. Begum, A. Irfan, W. Wu, S. Shaukat and Z. H. Farooqi, *Appl. Organomet. Chem.*, 2021, **35**, e6405.
60 T. Zhang, L. Li, Z. Ye, Q. Yang, Y. Tian and X. Guo, *RSC Adv.*, 2018, **8**, 18252–18259.
61 N. Tan, C. Lee and P. Li, *Polymers*, 2016, **8**, 105.
62 A. Mohan, J. Peter, L. Rout, A. M. Thomas, S. Nagappan, S. Parambadath, W. Zhang, M. Selvaraj and C.-S. Ha, *Colloids Surf., A*, 2021, **611**, 125846.
63 C. Alarcón-Fernández, M. Doña, A. Tapia-Fernández, G. Villaverde, M. R. Lopez-Ramirez, J. M. López-Romero and R. Contreras-Caceres, *ACS Appl. Nano Mater.*, 2020, **3**, 8247–8256.
64 L. Tzounis, M. Doña, J. M. Lopez-Romero, A. Fery and R. Contreras-Caceres, *ACS Appl. Mater. Interfaces*, 2019, **11**, 29360–29372.
65 T. Curtis, A. K. Taylor, S. E. Alden, C. Swanson, J. Lo, L. Knight, A. Silva, B. D. Gates, S. R. Emory and D. A. Rider, *ACS Omega*, 2018, **3**, 10572–10588.
66 J. Hong, T. Wu, H. Wu, B. Zeng, S. Zeng, T. Chen, X. Wang, Z. Lu, C. Yuan, K. Balaji, D. F. S. Petri and L. Dai, *Chem. Eng. J.*, 2021, **407**, 127087.
67 N. George, J. Joy, B. Mathew and E. P. Koshy, *J. Sol-Gel Sci. Technol.*, 2023, **107**, 685–696.
68 B. Lin, Y. Wang, Y. Yao, L. Chen, Y. Zeng, L. Li, Z. Lin and L. Guo, *Anal. Chem.*, 2021, **93**, 16727–16733.
69 S. Yan, C. Jiang, J. Guo, Y. Fan and Y. Zhang, *Polymers*, 2019, **11**, 401.
70 S. Li, D. Lin, J. Zhou and L. Zha, *J. Phys. Chem. C*, 2016, **120**, 4902–4908.
71 T. Kamal, M. S. J. Khan, S. B. Khan, A. M. Asiri, M. T. S. Chani and M. W. Ullah, *J. Polym. Environ.*, 2020, **28**, 399–410.
72 Z. Iqbal, L. A. Shah, M. Sayed, A. Haleem and M. Siddiq, *J. Chil. Chem. Soc.*, 2016, **61**, 3061–3065.
73 H. Park, L. Srisombat, A. Jamison, T. Liu, M. Marquez, H. Park, S. Lee, T.-C. Lee and T. Lee, *Gels*, 2018, **4**, 28.
74 M. Wei and M. J. Serpe, *Part. Part. Syst. Charact.*, 2019, **36**, 1800326.
75 Y. Yang, J. Maldonado-Valderrama and A. Martín-Molina, *J. Mol. Liq.*, 2020, **303**, 112678.
76 V. Nigro, R. Angelini, B. Rosi, M. Bertoldo, E. Buratti, S. Casciardi, S. Sennato and B. Ruzicka, *J. Colloid Interface Sci.*, 2019, **545**, 210–219.
77 A. Haleem, S. B. Syaal, M. Ajmal, J. Ambreen, S. Rauf, N. Ali, S. Muhammad, A. Shah, M. A. Zia and M. Siddiq, *Korean J. Chem. Eng.*, 2020, **37**, 614–622.
78 L. A. Shah, J. Ambreen, I. Bibi, M. Sayed and M. Siddiq, *J. Chem. Soc. Pak.*, 2016, **38**, 850.
79 S. Ashraf, R. Begum, R. Rehan, W. Wu and Z. H. Farooqi, *J. Inorg. Organomet. Polym. Mater.*, 2018, **28**, 1872–1884.
80 N. S. Reddy, S. Eswaramma, I. Chung, K. S. V. K. Rao, P. Ramesh and A. Chandra Sekhar, *Int. J. Polym. Mater. Polym. Biomater.*, 2019, **68**, 870–880.

81 J. Cao, J. Li, Y. Chen, L. Zhang and J. Zhou, *Adv. Funct. Mater.*, 2018, **28**, 1800739.
82 L. Li, R. Niu and Y. Zhang, *RSC Adv.*, 2018, **8**, 12428–12438.
83 V. Melinte, L. Stroea, T. Buruiana and A. L. Chibac, *Eur. Polym. J.*, 2019, **121**, 109289.
84 S. Pandey, N. Son and M. Kang, *Int. J. Biol. Macromol.*, 2022, **210**, 300–314.
85 A. M. Atta, A. K. Gafer, H. A. Al-Lohedan, M. M. S. Abdullah, A. M. Tawfeek and A. O. Ezzat, *Molecules*, 2019, **24**, 3867.
86 P. Bhol, M. Mohanty and P. S. Mohanty, *J. Mol. Liq.*, 2021, **325**, 115135.
87 Z. H. Farooqi, R. Begum, K. Naseem, U. Rubab, M. Usman, A. Khan and A. Ijaz, *Russ. J. Phys. Chem. A*, 2016, **90**, 2600–2608.
88 M. Ajmal, S. Anwar, H. Naeem, M. A. Zia and M. Siddiq, *Polym. Eng. Sci.*, 2020, **60**, 2918–2929.
89 Y. Mao, H. Zhang, S. Ahmed, S. Li, S. Zhang and J. Wang, *Appl. Catal., B*, 2022, **314**, 121456.
90 A. K. Sarkar, A. Saha, L. Midya, C. Banerjee, N. Mandre, A. B. Panda and S. Pal, *ACS Sustain. Chem. Eng.*, 2017, **5**, 1881–1891.
91 Y. Feng, J. Yin, S. Liu, Y. Wang, B. Li and T. Jiao, *ACS Omega*, 2020, **5**, 3725–3733.
92 L. A. Shah, A. Haleem, M. Sayed and M. Siddiq, *J. Environ. Chem. Eng.*, 2016, **4**, 3492–3497.
93 K. Naseem, R. Begum, Z. H. Farooqi, W. Wu and A. Irfan, *Appl. Organomet. Chem.*, 2020, **34**, e5742.
94 S. Velpula, S. R. Beedu and K. Rupula, *Int. J. Biol. Macromol.*, 2021, **190**, 159–169.
95 A. Raza, S. Rauf Khan, S. Ali, S. Jamil and S. Bibi, *Inorg. Chem. Commun.*, 2023, **153**, 110851.
96 K. Naseem, Z. H. Farooqi, R. Begum, W. Wu, A. Irfan and A. G. Al-Sehemi, *Macromol. Chem. Phys.*, 2018, **219**, 1800211.
97 D. Parida, E. Moreau, R. Nazir, K. A. Salmeia, R. Frison, R. Zhao, S. Lehner, M. Jovic and S. Gaan, *J. Hazard. Mater.*, 2021, **416**, 126237.
98 Y. Li, M. Jiao, H. Zhao and M. Yang, *Sens. Actuators, B*, 2018, **273**, 133–142.
99 S. Batool, Z. Hussain, M. B. K. Niazi, U. Liaqat and M. Afzal, *J. Drug Delivery Sci. Technol.*, 2019, **52**, 403–414.
100 E. Jha, P. Patel, P. Kumari, K. K. Verma, P. K. Panda, P. S. Mohanty, S. Patro, R. S. Varma, Y. K. Mishra, N. K. Kaushik, M. Suar and S. K. Verma, *J. Environ. Chem. Eng.*, 2023, **11**, 111183.
101 L. Schnaider, Z. Toprakcioglu, A. Ezra, X. Liu, D. Bychenko, A. Levin, E. Gazit and T. P. J. Knowles, *Nano Lett.*, 2020, **20**, 1590–1597.
102 M. He, Q. Wang, R. Wang, Y. Xie, W. Zhao and C. Zhao, *ACS Appl. Mater. Interfaces*, 2017, **9**, 15962–15974.
103 F. Li, J. Tang, J. Geng, D. Luo and D. Yang, *Prog. Polym. Sci.*, 2019, **98**, 101163.
104 M. Sabzi, M. J. Afshari, M. Babaahmadi and N. Shafagh, *Colloids Surf., B*, 2020, **188**, 110757.
105 D. M. Suflet, I. Popescu, I. M. Pelin, D. L. Ichim, O. M. Daraba, M. Constantin and G. Fundueanu, *Pharmaceutics*, 2021, **13**, 1461.
106 M. Mofidfar, E. S. Kim, E. L. Larkin, L. Long, W. D. Jennings, S. Ahadian, M. A. Ghannoum and G. E. Wnek, *Micromachines*, 2019, **10**, 829.
107 M. T. S. Alcântara, N. Lincopan, P. M. Santos, P. A. Ramirez, A. J. C. Brant, H. G. Riella and A. B. Lugão, *Radiat. Phys. Chem.*, 2020, **169**, 108777.
108 M. R. El-Aassar, O. M. Ibrahim, M. M. G. Fouda, H. Fakhry, J. Ajarem, S. N. Maodaa, A. A. Allam and E. E. Hafez, *Carbohydr. Polym.*, 2021, **255**, 117484.
109 H. E. Salama, G. R. Saad and M. W. Sabaa, *J. Biomater. Sci., Polym. Ed.*, 2016, **27**, 1880–1898.
110 C. Ryan, E. Alcock, F. Buttimer, M. Schmidt, D. Clarke, M. Pemble and M. Bardosova, *Sci. Technol. Adv. Mater.*, 2017, **18**, 528–540.
111 N. S. V. Capanema, I. C. Carvalho, A. A. P. Mansur, S. M. Carvalho, A. P. Lage and H. S. Mansur, *ACS Appl. Nano Mater.*, 2019, **2**, 7393–7408.